

Estimating the Information Rate of a Channel with Classical Input and Output and a Quantum State

Michael X. Cao and Pascal O. Vontobel
 Department of Information Engineering
 The Chinese University of Hong Kong
 {m.x.cao, pascal.vontobel}@ieee.org

Abstract—We consider the problem of transmitting classical information over a time-invariant channel with memory. A popular class of time-invariant channels with memory are finite-state-machine channels, where a classical state evolves over time and governs the relationship between the classical input and the classical output of the channel. For such channels, various techniques have been developed for estimating and bounding the information rate.

In this paper we consider a class of time-invariant channels where a quantum state evolves over time and governs the relationship between the classical input and the classical output of the channel. We propose algorithms for estimating and bounding the information rate of such channels. In particular, we discuss suitable graphical models for doing the relevant computations.

I. INTRODUCTION

In this section, we first review some results about classical channels, in particular channels with an evolving classical state. Afterwards, we discuss channels with an evolving quantum state. Finally, we highlight the contributions of this paper.

A. Information Rates of Classical Channels

The information rate of a classical point-to-point channel characterizes the amount of classical information per channel use that can be transmitted reliably with the help of this channel. A particularly interesting class of channels are discrete memoryless channels (DMCs). A DMC is characterized by a channel input alphabet \mathcal{X} , a channel output alphabet \mathcal{Y} , and a channel law $W(y|x)$, where the latter equals the probability of receiving y upon sending x . (Here and in the following, we assume that \mathcal{X} and \mathcal{Y} are finite sets.) As is well known [1], the information rate $I(Q, W)$ of a DMC is given by

$$I(Q, W) = \sum_{x \in \mathcal{X}} \sum_{y \in \mathcal{Y}} Q(x) W(y|x) \log \left(\frac{W(y|x)}{(QW)(y)} \right), \quad (1)$$

where Q is some probability mass function (pmf) on \mathcal{X} and $(QW)(y) \triangleq \sum_{x \in \mathcal{X}} Q(x) W(y|x)$. Recall that in order to achieve this information rate, one needs to design a suitable encoder and a suitable decoder for some suitably chosen codebook where the distribution of the entries of the codewords equals Q . Because of the simplicity of the expression in (1), the information $I(Q, W)$ can be efficiently computed for any given Q .¹

¹Note that even the maximization of $I(Q, W)$ over all pmfs over \mathcal{X} can be done efficiently [2], [3]. The maximal information rate is known as the capacity of the DMC and the maximizing Q is known as the capacity-achieving input distribution.

Example 1. For any $0 \leq p \leq 1$, the binary symmetric channel with cross-over probability p , henceforth called $BSC(p)$, is a DMC with $\mathcal{X} \triangleq \{0, 1\}$, $\mathcal{Y} = \{0, 1\}$, $W(0|0) = 1 - p$, $W(1|0) = p$, $W(0|1) = p$, and $W(1|1) = 1 - p$. If $Q(0) = Q(1) = 1/2$, then its information rate is $I(Q, W) = 1 - h_2(p)$ bits per channel use, where h_2 is the binary entropy function.

We proceed to channels with memory, in particular to stationary ergodic channels with input alphabet \mathcal{X} and output alphabet \mathcal{Y} . Let W denote the channel law of such a channel. Under suitable conditions [1], the information rate is given by $I(Q, W) = \lim_{n \rightarrow \infty} \frac{1}{n} I(X_1, X_2, \dots, X_n; Y_1, Y_2, \dots, Y_n)$, where $X \triangleq (X_1, X_2, \dots)$ is the channel input process characterized by some stationary ergodic law Q , and where $Y \triangleq (Y_1, Y_2, \dots)$ is the channel output process.

For such channels, computing the information rate, let alone the capacity, is much more challenging than for DMCs. Namely, except for very special cases, there are no single-letter or other simple expressions for information rates available, and so, most of the time, one needs to rely on upper and lower bounds and/or on stochastic techniques for estimating the information rate.

Notably, in the case of finite-state-machine channels (FSMCs) [1], *i.e.*, channels with a finite classical state, efficient stochastic techniques have been developed for estimating the information rate [4], [5], [6]. (For these techniques, under mild conditions, the numerical estimate of the information rate converges with probability one to the true value when the length of the channel input sequence goes to infinity.) However, even for FSMCs, maximizing the information rate is much more challenging than maximizing the information rate of DMCs [7].

Example 2. A notable example of an FSMC is the Gilbert–Elliott channel [8], which can be either in the so-called “good” state or in the so-called “bad” state. If the channel is in the “good” state, then it behaves like a $BSC(p_g)$, but if the channel is in the “bad” state, then it behaves like a $BSC(p_b)$, where usually $|p_b - \frac{1}{2}| < |p_g - \frac{1}{2}|$. The state process itself is a first-order stationary ergodic Markov process which is independent of the input process.² (For more details, see, e.g., the discussions in [7], [9].)

²The independence of the state process on the input process is a particular feature of the Gilbert–Elliott channel. In general, the state process of a finite-state channel can depend on the input process.

For FSMCs with large state spaces, the above-mentioned information rate estimation techniques can be time-consuming and so stochastic techniques to estimate upper and lower bounds have proven useful [4], [9]. These bounding techniques are based on a so-called auxiliary FSMC, which is a low-complexity approximation of the true FSMC. Interestingly enough, the lower bounds represent achievable rates under mismatched decoding, where the decoder bases its computations not on the true FSMC but on the auxiliary FSMC [10]. (See the paper [9] for a more detailed discussion of this topic and for further references.)

B. Information Rates of Channels with a Quantum State — Paper Overview

In this paper we consider the problem of transmitting classical information over a channel with an evolving *quantum* state. A particular instance of such a channel is as follows:

- The state is given by some quantum system, called the state quantum system, whose position in space does not change and which, if left by itself, evolves according to some Hamiltonian \mathcal{H}_s .
- Alice wants to transmit some classical information to Bob. To this end, she uses a classical code to encode her information word $\mathbf{u} = (u_1, u_2, \dots, u_k) \in \mathcal{U}^k$ into a codeword $\mathbf{x} = (x_1, x_2, \dots, x_n) \in \mathcal{X}^n$.
- At time instance ℓ , Alice encodes $x_\ell \in \mathcal{X}$ as a particular state of some quantum system, called the ℓ -th transmit quantum system, which she sends to Bob.
- On the way to Bob, the ℓ -th transmit quantum system interacts with the state quantum system.
- Bob receives the ℓ -th transmit quantum system and performs a quantum measurement resulting in some value $y_\ell \in \mathcal{Y}$.
- After receiving $\mathbf{y} = (y_1, y_2, \dots, y_n) \in \mathcal{Y}^n$, Bob decodes \mathbf{y} toward obtaining an estimate $\hat{\mathbf{u}}$ of \mathbf{u} .

This setup is vaguely inspired by the setup in Fig. 4 of [11]. Note that the setup therein was *not* for data communication, but for manipulating and measuring what we call here the state quantum system.

In this paper, we discuss algorithms for estimating and lower bounding the information rate of such channels with an evolving quantum state (see Section III). Toward this end, we introduce suitable graphical models for visualizing and doing the relevant computations (see Section II). Finally, we present some numerical results (see Section IV).

C. References with Background Information

In the following, we assume that the reader is familiar with the very basics of quantum information processing (see, e.g., the excellent book Nielsen and Chuang [12] for an introduction). For a general introduction to quantum channels with memory, we refer to the survey papers by Kretschmann and Werner [13] and by Caruso *et al.* [14].

Moreover, some familiarity with graphical models (like factor graphs) [15], [16], [17] and with techniques for estimating the information rate of a classical FSMC as presented

in [4], [9] will be beneficial. Recall that graphical models are a popular approach for representing multivariate functions with non-trivial factorizations and for doing computations like marginalization [15], [16], [17]. In particular, graphical models can be used to represent joint probability mass functions (pmfs) / probability density functions (pdfs). In the present paper we will heavily rely on the papers [18], [19], which discussed an approach for using normal factor graphs (NFGs) for representing functions that typically appear when doing computations w.r.t. some quantum systems. Probabilities of interest are then obtained by suitably applying the sum-product algorithm / applying the closing-the-box operation.

II. CHANNELS WITH CLASSICAL OR QUANTUM STATES AND THEIR GRAPHICAL MODELS

We first review NFGs that were used in [4] in the context of estimating the information rate of channels with an evolving classical state. Afterwards, we will show NFGs that we can use for estimating the information rate of channels with an evolving quantum state.

A. Channels with a Classical State

Fig. 1 shows the NFG that was used in [4] in the context of estimating the information rate of channels with a classical state. Let $g(\mathbf{x}, \mathbf{y}, \tilde{\mathbf{s}})$ denote the global function of this NFG (*i.e.*, the multivariate function represented by this NFG), where $\mathbf{x} \triangleq (x_1, \dots, x_n)$, $\mathbf{y} \triangleq (y_1, \dots, y_n)$, and $\tilde{\mathbf{s}} \triangleq (\tilde{s}_0, \tilde{s}_1, \dots, \tilde{s}_n)$. Some comments:

- The part of the NFG inside the blue box represents the input process $Q(\mathbf{x})$. Here, for simplicity, the input process is an i.i.d. process characterized by the pmf p_X , *i.e.*, $Q(\mathbf{x}) = \prod_{\ell=1}^n p_X(x_\ell)$.
- The part of the NFG inside the red box represents $W(\mathbf{y}, \tilde{\mathbf{s}}|\mathbf{x})$, *i.e.*, the probability of \mathbf{y} and $\tilde{\mathbf{s}}$ given \mathbf{x} . After applying the closing-the-box operation, *i.e.*, after summing over all the variables associated with edges completely inside the red box, we obtain the channel law $W(\mathbf{y}|\mathbf{x}) \triangleq \sum_{\tilde{\mathbf{s}}} W(\mathbf{y}, \tilde{\mathbf{s}}|\mathbf{x})$.
- The function $W(\mathbf{y}, \tilde{\mathbf{s}}|\mathbf{x})$ decomposes as $W(\mathbf{y}, \tilde{\mathbf{s}}|\mathbf{x}) = p_{\tilde{s}_0}(\tilde{s}_0) \cdot \prod_{\ell=1}^n W(\tilde{s}_\ell, y_\ell | \tilde{s}_{\ell-1}, x_\ell)$. Here, $p_{\tilde{s}_0}$ is a pmf and $W(\tilde{s}_\ell, y_\ell | \tilde{s}_{\ell-1}, x_\ell)$ is assumed to be a conditional pmf:

$$\forall \tilde{s}_\ell, y_\ell, \tilde{s}_{\ell-1}, x_\ell : W(\tilde{s}_\ell, y_\ell | \tilde{s}_{\ell-1}, x_\ell) \geq 0, \quad (2)$$

$$\forall \tilde{s}_{\ell-1}, x_\ell : \sum_{\tilde{s}_\ell, y_\ell} W(\tilde{s}_\ell, y_\ell | \tilde{s}_{\ell-1}, x_\ell) = 1. \quad (3)$$

With this, one can verify that the NFG in Fig. 1 has the following properties. (Most of these properties are in contrast to the properties of the upcoming NFG that we will use for channels with a quantum state.)

- The global function $g(\mathbf{x}, \mathbf{y}, \tilde{\mathbf{s}})$ is a pmf over \mathbf{x} , \mathbf{y} , and $\tilde{\mathbf{s}}$.
- The function $g(\mathbf{x}, \mathbf{y}) \triangleq \sum_{\tilde{\mathbf{s}}} g(\mathbf{x}, \mathbf{y}, \tilde{\mathbf{s}})$, which is obtained by summing the global function over $\tilde{\mathbf{s}}$, represents the corresponding marginal pmf over \mathbf{x} and \mathbf{y} . The function $g(\tilde{\mathbf{s}}) \triangleq \sum_{\mathbf{x}, \mathbf{y}} g(\mathbf{x}, \mathbf{y}, \tilde{\mathbf{s}})$, which is obtained by summing the global function over \mathbf{x} and \mathbf{y} , represents the corresponding marginal pmf over $\tilde{\mathbf{s}}$. *Etc.*

— See Appendix A for additional comments. —

B. Channels with a Quantum State

We now turn our attention to channels with an evolving quantum state. In this case, it is in general *not* possible to come up with an NFG that has a “nice” factorization and that has the properties listed at the end of Section II-A. However, note that we “only” need an NFG with a global function $g(\mathbf{x}, \mathbf{y}, \dots)$ which has the property that if we sum over all variables except \mathbf{x} and \mathbf{y} , then we obtain a pmf over \mathbf{x} and \mathbf{y} . In particular, we do *not* need $g(\mathbf{x}, \mathbf{y}, \dots)$ to have the property that if we sum over \mathbf{x} and \mathbf{y} then the resulting function is a pmf over the remaining variables.

Consider an NFG with global function $g(\mathbf{x}, \mathbf{y}, \mathbf{s}, \mathbf{s}')$, where $\mathbf{x} \triangleq (x_1, \dots, x_n)$, $\mathbf{y} \triangleq (y_1, \dots, y_n)$, $\mathbf{s} \triangleq (s_0, s_1, \dots, s_n)$, and $\mathbf{s}' \triangleq (s'_0, s'_1, \dots, s'_n)$. Define $g(\mathbf{x}, \mathbf{y}) \triangleq \sum_{\mathbf{s}, \mathbf{s}'} g(\mathbf{x}, \mathbf{y}, \mathbf{s}, \mathbf{s}')$. The above-mentioned conditions mean that $g(\mathbf{x}, \mathbf{y})$ must be a pmf over \mathbf{x} and \mathbf{y} , but $g(\mathbf{x}, \mathbf{y}, \mathbf{s}, \mathbf{s}')$ need *not* be a pmf over $\mathbf{x}, \mathbf{y}, \mathbf{s}$, and \mathbf{s}' . In particular, $g(\mathbf{s}, \mathbf{s}') \triangleq \sum_{\mathbf{x}, \mathbf{y}} g(\mathbf{x}, \mathbf{y}, \mathbf{s}, \mathbf{s}')$ need *not* be a pmf over \mathbf{s} and \mathbf{s}' .

As it happens to be, considering NFGs whose global function $g(\mathbf{x}, \mathbf{y}, \mathbf{s}, \mathbf{s}')$ satisfies

$$\forall \mathbf{x}, \mathbf{y}, \mathbf{s}, \mathbf{s}' : g(\mathbf{x}, \mathbf{y}, \mathbf{s}, \mathbf{s}') \in \mathbb{C} , \quad (4)$$

$$\forall \mathbf{x}, \mathbf{y}, \mathbf{s}, \mathbf{s}' : g(\mathbf{x}, \mathbf{y}, \mathbf{s}, \mathbf{s}') = \overline{g(\mathbf{x}, \mathbf{y}, \mathbf{s}', \mathbf{s})} , \quad (5)$$

$$\sum_{\mathbf{x}, \mathbf{y}, \mathbf{s}, \mathbf{s}'} g(\mathbf{x}, \mathbf{y}, \mathbf{s}, \mathbf{s}') = 1 , \quad (6)$$

$$\forall \mathbf{x}, \mathbf{y} : g(\mathbf{x}, \mathbf{y}) \in \mathbb{R}_{\geq 0} , \quad (7)$$

$$\sum_{\mathbf{x}, \mathbf{y}} g(\mathbf{x}, \mathbf{y}) = 1 , \quad (8)$$

is general enough in order to capture quantum phenomena and to represent the associated computations with the help of NFGs that have a “nice” factorization [19].³

With suitably chosen local function nodes, the NFG in Fig. 2 is an NFG that satisfies (4)–(8). Specifically, it suffices to impose the following requirements on the local function nodes:

- The input process is an i.i.d. process characterized by the pmf p_X . (This is for simplicity only; more complicated processes could be used.)
- In order to show the constraints on the function W , it is beneficial to write its arguments as follows: $W^{(y_\ell|x_\ell)}(s_{\ell-1}, s_\ell; s'_{\ell-1}, s'_\ell)$. Moreover, for any fixed x_ℓ and y_ℓ , we denote by $W^{(y_\ell|x_\ell)}$ the matrix with row labels $(s_{\ell-1}, s_\ell)$, with column labels $(s'_{\ell-1}, s'_\ell)$, and with entries $W^{(y_\ell|x_\ell)}(s_{\ell-1}, s_\ell; s'_{\ell-1}, s'_\ell)$. With this, W has to satisfy

$$\forall x_\ell, y_\ell : W^{(y_\ell|x_\ell)} \text{ is a p.s.d. matrix (over } \mathbb{C} \text{)} , \quad (9)$$

$$\forall x_\ell, s_{\ell-1}, s'_{\ell-1} : \sum_{s_\ell, s'_\ell, y_\ell} W^{(y_\ell|x_\ell)}(s_{\ell-1}, s_\ell; s'_{\ell-1}, s'_\ell) \cdot \delta(s'_\ell, s_\ell) = \delta(s'_{\ell-1}, s_{\ell-1}) , \quad (10)$$

where p.s.d. stands for positive semi-definite and where δ is the Kronecker-delta function. Note that condition (10)

³The over-line in (5) denotes complex conjugation. Note that condition (8) is redundant given condition (6), but we display it because of its importance.

can be visualized as shown in Fig. 3, where applying a closing-the-box operation [19] to the NFG on the left-hand side results in the NFG on the right-hand side. (On the side, we note that with the above ordering of the entries, for every x_ℓ the matrix $\sum_{y_\ell} W^{(y_\ell|x_\ell)}$ is known to be in Choi-matrix-representation form or in dynamical-matrix-representation form [20].)

- The initial quantum state (s_0, s'_0) is characterized by the complex-valued function ρ^{S_0} , which, when written as a matrix, is p.s.d. (over \mathbb{C}) and has trace one.

One can verify that these constraints on the local functions of the NFG in Fig. 2 lead to a global function $g(\mathbf{x}, \mathbf{y}, \mathbf{s}, \mathbf{s}')$ which satisfies (4)–(8).

— See Appendix B for additional comments. —

Example 3. As a particular example of a channel with a quantum state, we propose a quantum version of the classical Gilbert–Elliott channel, henceforth called the *Quantum Gilbert–Elliott channel*. We define this channel by specifying the NFG as in Fig. 4, which, upon closing-the-box results in a function node that can be used as $W^{(y_\ell|x_\ell)}(s_{\ell-1}, s_\ell; s'_{\ell-1}, s'_\ell)$ in Fig. 2. The NFG in Fig. 4 stems from the following considerations. (Recall the communication setup from Section I-B.)

- $\mathcal{X} \triangleq \{0, 1\}$, $\mathcal{Y} \triangleq \{0, 1\}$, $\mathcal{S} \triangleq \mathcal{S}' \triangleq \{0, 1\}$.
- The state quantum system is some qubit.
- The ℓ -th transmit quantum system is some qubit.
- At time index ℓ , Alice encodes x_ℓ into state $\rho_{x_\ell}^A$ of the ℓ -th transmit quantum system, where the matrix version of $\rho_{x_\ell}^A$ is a p.s.d. matrix with trace one. Specifically, for the communication setups in Section IV we choose $\rho_0^A = \begin{pmatrix} 1 & 0 \\ 0 & 0 \end{pmatrix}$ and $\rho_1^A = \begin{pmatrix} 0 & 0 \\ 0 & 1 \end{pmatrix}$.
- Alice sends the ℓ -th transmit quantum system to Bob. On its way it interacts with the state quantum system. This interaction is described in terms of an operator-sum representation [12, Chap. 8] based on matrices E_{k_ℓ} , $k_\ell \in \{0, 1\}$, where

$$E_0 \triangleq \begin{bmatrix} \sqrt{1-p_g} & 0 & 0 & 0 \\ 0 & \sqrt{1-p_g} & 0 & 0 \\ 0 & 0 & \sqrt{1-p_b} & 0 \\ 0 & 0 & 0 & \sqrt{1-p_b} \end{bmatrix}, \quad E_1 \triangleq \begin{bmatrix} 0 & \sqrt{p_g} & 0 & 0 \\ \sqrt{p_g} & 0 & 0 & 0 \\ 0 & 0 & 0 & \sqrt{p_b} \\ 0 & 0 & \sqrt{p_b} & 0 \end{bmatrix}.$$

- Bob performs a quantum measurement [12, Chap. 2] defined by measurement operators $\{M_{y_\ell}\}_{y_\ell \in \mathcal{Y}}$ on the ℓ -th transmit quantum system. Specifically, for the communication setups in Section IV we choose $M_0 = \begin{pmatrix} 1 & 0 \\ 0 & 0 \end{pmatrix}$ and $M_1 = \begin{pmatrix} 0 & 0 \\ 0 & 1 \end{pmatrix}$.
- Between two transmissions, the evolution of the state quantum system is described by a unitary matrix U that is derived from the Hamiltonian \mathcal{H}_s and the time difference between two transmissions.

Note that for function nodes in the NFG in Fig. 4 that were specified in terms of a matrix, we use a dot to denote the variable that corresponds to the row index of the matrix. (In the case of the function nodes E_{k_ℓ} and $E_{k_\ell}^H$, two variables jointly correspond to the row index of the matrix.)

— See Appendix C for additional comments. —

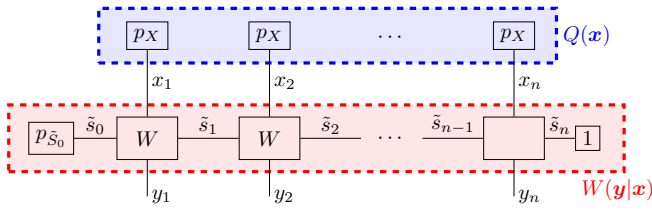


Fig. 1. Channel with a classical state: joint NFG for input process $Q(x)$ (blue box) and channel law $W(y|x)$ (red box), after closing-the-box.

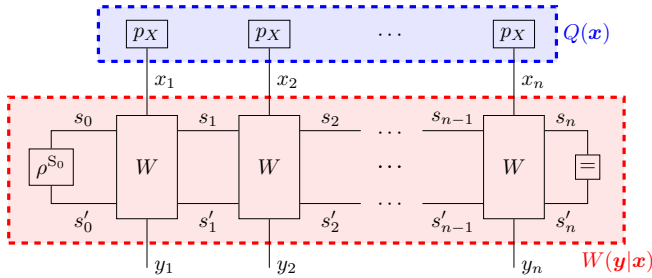


Fig. 2. Channel with a quantum state: joint NFG for input process $Q(x)$ (blue box) and channel law $W(y|x)$ (red box), after closing-the-box.

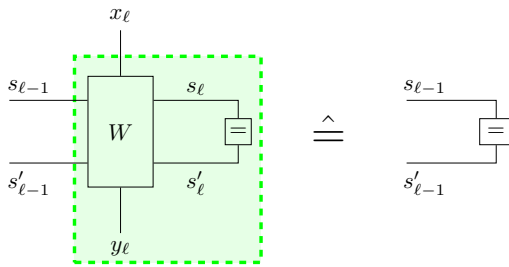


Fig. 3. NFGs visualizing the constraint (10) that W has to satisfy. Namely, after applying the closing-the-box operation to the NFG on the left-hand side, one has to obtain the NFG on the right-hand side. (Note that on the right-hand side, the edge corresponding to x_ℓ has been omitted because it is not connected to any function node.)

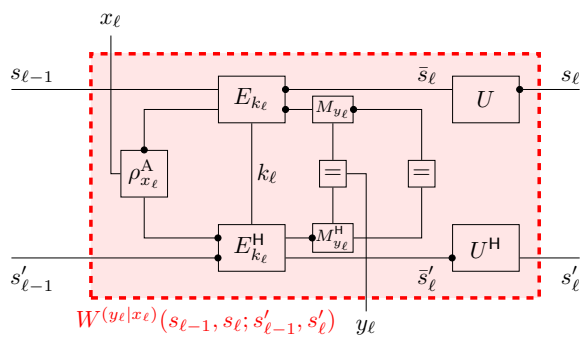


Fig. 4. Internal details of $W^{(y_\ell|x_\ell)}(s_{l-1}, s_\ell; s'_{l-1}, s'_\ell)$ for the Quantum Gilbert-Elliott Channel.

III. INFORMATION RATE ESTIMATION

Recall that the approach of [4] for estimating information rates of FSMCs is based on the Shannon–McMillan–Breiman theorem (see, *e.g.*, [21]) and suitable generalizations. Namely, the information rate

$$I(X; Y) = H(X) + H(Y) - H(X, Y)$$

of a channel with a classical state can be estimated as follows:

- 1) Randomly generate a channel input sequence $\tilde{x} = (\tilde{x}_1, \tilde{x}_2, \dots, \tilde{x}_n)$ according to the law Q .
- 2) Based on this channel input sequence, randomly generate a channel output sequence $\tilde{y} = (\tilde{y}_1, \tilde{y}_2, \dots, \tilde{y}_n)$.
- 3) Estimate $H(X)$, $H(Y)$, $H(X, Y)$ by computing $-\frac{1}{n} \log(g(\tilde{x}))$, $-\frac{1}{n} \log(g(\tilde{y}))$, $-\frac{1}{n} \log(g(\tilde{x}, \tilde{y}))$, where $g(\tilde{x}) = \sum_{\mathbf{y}, \tilde{s}} g(\tilde{x}, \mathbf{y}, \tilde{s})$, $g(\tilde{y}) = \sum_{\mathbf{x}, \tilde{s}} g(\mathbf{x}, \tilde{y}, \tilde{s})$, $g(\tilde{x}, \tilde{y}) = \sum_{\tilde{s}} g(\tilde{x}, \tilde{y}, \tilde{s})$.
- 4) Combine the above estimates to obtain an estimate of $I(X; Y)$.

Thanks to the close relationship between the NFG in Fig. 1 and the NFG in Fig. 2, it is *formally* straightforward to generalize the above procedure to channels with a quantum state. Namely, one simply has to replace Step 3) by Step 3'), where

- 3') Estimate $H(X)$, $H(Y)$, $H(X, Y)$ by computing $-\frac{1}{n} \log(g(\tilde{x}))$, $-\frac{1}{n} \log(g(\tilde{y}))$, $-\frac{1}{n} \log(g(\tilde{x}, \tilde{y}))$, where $g(\tilde{x}) = \sum_{\mathbf{y}, \mathbf{s}, \mathbf{s}' } g(\tilde{x}, \mathbf{y}, \mathbf{s}, \mathbf{s}')$, $g(\tilde{y}) = \sum_{\mathbf{x}, \mathbf{s}, \mathbf{s}' } g(\mathbf{x}, \tilde{y}, \mathbf{s}, \mathbf{s}')$, $g(\tilde{x}, \tilde{y}) = \sum_{\mathbf{s}, \mathbf{s}' } g(\tilde{x}, \tilde{y}, \mathbf{s}, \mathbf{s}')$.

In order to efficiently compute all the relevant quantities, one can apply suitable closing-the-box operations as in [19], in particular as in Section IV of [19]. This is equivalent to applying the sum-product algorithm on a modified version of the underlying NFG, where edges are suitably merged so that the modified NFG does not contain cycles and so that the computed marginals are exact.

— See Appendix D for additional comments. —

IV. NUMERICAL EXAMPLES

In Figs. 5–8, we present some numerical information rate (IR) estimates for various setups of the Quantum Gilbert–Elliott channel where the channel input process is an i.i.d. process with $p_X(0) = p_X(1) = 1/2$. (See the figure captions for further details.) In Figs. 5–8, we also show some auxiliary-channel-based information rate lower bound estimates that are based on auxiliary channels with a classical state [4]. These auxiliary channels were optimized with the help of the techniques in [9]. Finally, Fig. 6 includes an auxiliary-channel-based information rate lower bound estimate that is based on an auxiliary channel with a quantum state. As already emphasized beforehand, these lower bounds represent rates that are achievable with the help of a mismatched decoder [10].

— See Appendix E for additional comments. —

ACKNOWLEDGMENT

It is a great pleasure to acknowledge discussions on topics related to this paper with Andi Loeliger.

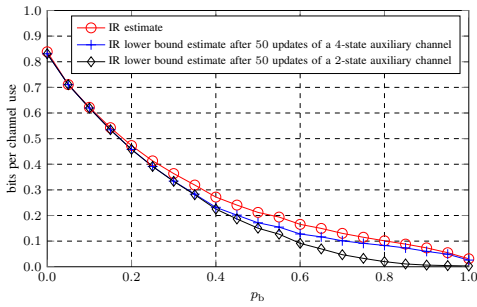


Fig. 5. Quantum Gilbert-Elliott Channel: $p_g = 0.05$ is fixed; p_b varies from 0 to 1; $U = \exp(-i\alpha H)$, where H is some fixed Hermitian matrix and where $\alpha = 1$ is fixed; $n = 10^5$.

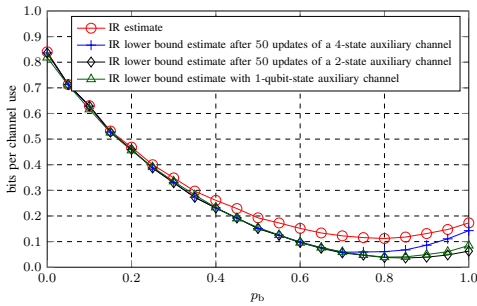


Fig. 6. Variant of the Quantum Gilbert-Elliott Channel where the state quantum system consists of two qubits whose evolution is described by U , but where only one of the qubits interacts directly with the transmit quantum system: $p_g = 0.05$ is fixed; p_b varies from 0 to 1; $U = \exp(-i\alpha H)$, where H is some fixed Hermitian matrix and where $\alpha = 1.2$ is fixed; $n = 10^5$.

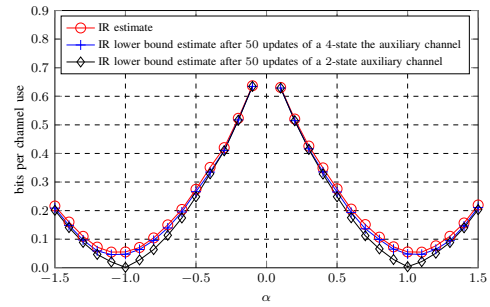


Fig. 7. Quantum Gilbert-Elliott Channel: $p_g = 0.05$ is fixed; $p_b = 0.95$ is fixed; $U = \exp(-i\alpha H)$, where H is the same Hermitian matrix as in Fig. 5 and where α varies from -1.5 to $+1.5$; $n = 10^5$. (No information rate estimates are included for α around 0 because of slow mixing of the channel.)

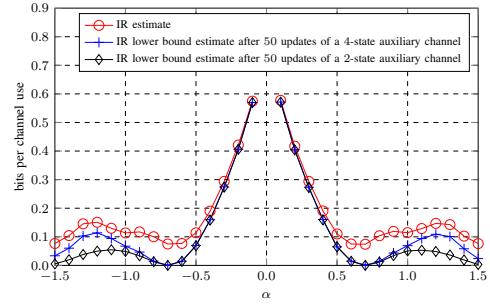


Fig. 8. Same variant of the Quantum Gilbert-Elliott Channel as in Fig. 6: $p_g = 0.05$ is fixed; $p_b = 0.95$ is fixed; $U = \exp(-i\alpha H)$, where H is the same Hermitian matrix as in Fig. 6 and where α varies from -1.5 to $+1.5$; $n = 10^5$. (No information rate estimates are included for α around 0 because of slow mixing of the channel.)

REFERENCES

- [1] R. G. Gallager, *Information Theory and Reliable Communication*. New York: Wiley, 1968.
- [2] S. Arimoto, "An algorithm for computing the capacity of arbitrary memoryless channels," *IEEE Trans. Inf. Theory*, vol. 18, no. 1, pp. 14–20, Jan. 1972.
- [3] R. E. Blahut, "Computation of channel capacity and rate distortion functions," *IEEE Trans. Inf. Theory*, vol. 18, no. 4, pp. 460–473, Jul. 1972.
- [4] D. M. Arnold, H.-A. Loeliger, P. O. Vontobel, A. Kavčić, and W. Zeng, "Simulation-based computation of information rates for channels with memory," *IEEE Trans. Inf. Theory*, vol. 52, no. 8, pp. 3498–3508, Aug. 2006.
- [5] V. Sharma and S. K. Singh, "Entropy and channel capacity in the regenerative setup with applications to Markov channels," in *Proc. IEEE Int. Symp. Inf. Theory*, Washington, D.C., June 24–29 2001, p. 283.
- [6] H. D. Pfister, J. B. Soriaga, and P. H. Siegel, "On the achievable information rates of finite-state ISI channels," in *Proc. IEEE Global Communications Conference*, San Antonio, TX, Nov. 2001, pp. 2992–2996.
- [7] P. O. Vontobel, A. Kavčić, D. M. Arnold, and H.-A. Loeliger, "A generalization of the Blahut-Arimoto algorithm to finite-state channels," *IEEE Trans. Inf. Theory*, vol. 54, no. 5, pp. 1887–1918, May 2008.
- [8] M. Mushkin and I. Bar-David, "Capacity and coding for the Gilbert-Elliott channel," *IEEE Trans. Inf. Theory*, vol. 35, no. 6, pp. 1277–1290, Nov. 1989.
- [9] P. Sadeghi, P. O. Vontobel, and R. Shams, "Optimization of information rate upper and lower bounds for channels with memory," *IEEE Trans. Inf. Theory*, vol. 55, no. 2, pp. 663–688, Feb. 2009.
- [10] A. Ganti, A. Lapidoth, and I. E. Telatar, "Mismatched decoding revisited: general alphabets, channels with memory, and the wide-band limit," *IEEE Trans. Inf. Theory*, vol. 46, no. 7, pp. 2315–2328, 2000.
- [11] Royal Swedish Academy of Sciences, "Measuring and manipulating individual quantum systems," *Scientific Background on the Nobel Prize in Physics awarded to Serge Haroche and David J. Wineland*, 2012, https://www.nobelprize.org/nobel_prizes/physics/laureates/2012/advanced.html.
- [12] M. A. Nielsen and I. L. Chuang, *Quantum Computation and Quantum Information*. Cambridge, UK: Cambridge University Press, 2000.
- [13] D. Kretschmann and R. F. Werner, "Quantum channels with memory," *Phys. Rev. A*, vol. 72, no. 062323, pp. 1–19, 2005.
- [14] F. Caruso, V. Giovannetti, C. Lupo, and S. Mancini, "Quantum channels and memory effects," *Rev. Mod. Phys.*, vol. 86, pp. 1203–1259, Oct.–Dec. 2014.
- [15] F. R. Kschischang, B. J. Frey, and H.-A. Loeliger, "Factor graphs and the sum-product algorithm," *IEEE Trans. Inf. Theory*, vol. 47, no. 2, pp. 498–519, Feb. 2001.
- [16] G. D. Forney, Jr., "Codes on graphs: normal realizations," *IEEE Trans. Inf. Theory*, vol. 47, no. 2, pp. 520–548, Feb. 2001.
- [17] H.-A. Loeliger, "An introduction to factor graphs," *IEEE Sig. Proc. Mag.*, vol. 21, no. 1, pp. 28–41, Jan. 2004.
- [18] H.-A. Loeliger and P. O. Vontobel, "A factor-graph representation of probabilities in quantum mechanics," in *Proc. IEEE Int. Symp. Inf. Theory*, Cambridge, MA, USA, Jul. 1–6 2012, pp. 656–660.
- [19] —, "Factor graphs for quantum probabilities," *submitted to IEEE Trans. Inf. Theory*, available online under <http://arxiv.org/abs/1508.00689>, Aug. 2015.
- [20] C. J. Wood, J. D. Biamonte, and D. G. Cory, "Tensor networks and graphical calculus for open quantum systems," *Quantum Inf. and Comp.*, vol. 15, no. 9–10, pp. 759–811, 2015.
- [21] T. M. Cover and J. A. Thomas, *Elements of Information Theory*. New York: John Wiley & Sons Inc., 1991.
- [22] Y. Ephraim and N. Merhav, "Hidden Markov processes," *IEEE Trans. Inf. Theory*, vol. 48, no. 6, pp. 1518–1569, Jun. 2002.

NOTATION

In these appendices, we will use $\mathbf{x}_{\ell_1}^{\ell_2}$ to denote the vector $(x_{\ell_1}, \dots, x_{\ell_2})$, $\mathbf{y}_{\ell_1}^{\ell_2}$ to denote the vector $(y_{\ell_1}, \dots, y_{\ell_2})$, etc., where ℓ_1 and ℓ_2 are integers satisfying $\ell_1 \leq \ell_2$.

APPENDIX A

SUPPLEMENTARY NOTES FOR SECTION II-A

The main purpose of this appendix is to prove Lemma 1 (see below) about the global function of the NFG in Fig. 1, which is associated with a classical channel with memory.

Let $g(\mathbf{x}_1^n, \mathbf{y}_1^n, \tilde{\mathbf{s}}_0^n)$ be the global function of the NFG in Fig. 1, *i.e.*,

$$g(\mathbf{x}_1^n, \mathbf{y}_1^n, \tilde{\mathbf{s}}_0^n) \triangleq p_{\tilde{\mathbf{s}}_0}(\tilde{\mathbf{s}}_0) \cdot \prod_{\ell=1}^n \left(p_X(x_\ell) \cdot W(\tilde{s}_\ell, y_\ell | \tilde{s}_{\ell-1}, x_\ell) \right). \quad (11)$$

Moreover, let $Q(\mathbf{x}_1^n)$ be obtained by a suitable closing-the-box operation around parts of the NFG in Fig. 1 (see the blue box in Fig. 1), *i.e.*,

$$Q(\mathbf{x}_1^n) \triangleq \prod_{\ell=1}^n p_X(x_\ell), \quad (12)$$

and let $W(\mathbf{y}_1^n | \mathbf{x}_1^n)$ be obtained by a suitable closing-the-box operation around parts of the NFG in Fig. 1 (see the red box in Fig. 1), *i.e.*,

$$W(\mathbf{y}_1^n | \mathbf{x}_1^n) \triangleq \sum_{\tilde{\mathbf{s}}_0^n} p_{\tilde{\mathbf{s}}_0}(\tilde{\mathbf{s}}_0) \cdot \prod_{\ell=1}^n W(\tilde{s}_\ell, y_\ell | \tilde{s}_{\ell-1}, x_\ell). \quad (13)$$

(Note that here the closing-the-box operation for the blue box is trivial in the sense that there are no edges completely inside the blue box, and so there are no variables to sum over.)

Recall that the factorization of $g(\mathbf{x}_1^n, \mathbf{y}_1^n, \tilde{\mathbf{s}}_0^n)$ in (11) follows from the following assumptions on our source/channel model:

- The input process is an i.i.d. process.
- Conditioned on $\tilde{s}_{\ell-1}$ and x_ℓ , the channel state \tilde{s}_ℓ and channel output y_ℓ are conditionally independent of $\tilde{s}_0^{\ell-2}$, $\mathbf{x}_1^{\ell-1}$, and $\mathbf{y}_1^{\ell-1}$.

For more context and further details, we refer to [1]. (Note that what we call finite-state-machine channels (FSMCs) are called finite-state channels in [1].)

Lemma 1. *Assume that the channel model W is such that (2) and (3) hold. Then the function $g(\mathbf{x}_1^n, \mathbf{y}_1^n, \tilde{\mathbf{s}}_0^n)$ is a pmf over \mathbf{x}_1^n , \mathbf{y}_1^n , and $\tilde{\mathbf{s}}_0^n$, *i.e.*,*

$$\forall \mathbf{x}_1^n, \mathbf{y}_1^n, \tilde{\mathbf{s}}_0^n : g(\mathbf{x}_1^n, \mathbf{y}_1^n, \tilde{\mathbf{s}}_0^n) \geq 0, \quad (14)$$

$$\sum_{\mathbf{x}_1^n, \mathbf{y}_1^n, \tilde{\mathbf{s}}_0^n} g(\mathbf{x}_1^n, \mathbf{y}_1^n, \tilde{\mathbf{s}}_0^n) = 1. \quad (15)$$

Moreover, the function $Q(\mathbf{x}_1^n)$ is a pmf over \mathbf{x}_1^n , and the function $W(\mathbf{y}_1^n | \mathbf{x}_1^n)$ is a conditional pmf over \mathbf{y}_1^n given \mathbf{x}_1^n .

Proof. The fact that $g(\mathbf{x}_1^n, \mathbf{y}_1^n, \tilde{\mathbf{s}}_0^n) \geq 0$ for all $(\mathbf{x}_1^n, \mathbf{y}_1^n, \tilde{\mathbf{s}}_0^n)$ follows immediately from (11) and (2). On the other hand,

the fact that $\sum_{\mathbf{x}_1^n, \mathbf{y}_1^n, \tilde{\mathbf{s}}_0^n} g(\mathbf{x}_1^n, \mathbf{y}_1^n, \tilde{\mathbf{s}}_0^n) = 1$ can be shown by using (3) repeatedly. Namely,

$$\begin{aligned} & \sum_{\mathbf{x}_1^n, \mathbf{y}_1^n, \tilde{\mathbf{s}}_0^n} g(\mathbf{x}_1^n, \mathbf{y}_1^n, \tilde{\mathbf{s}}_0^n) \\ &= \sum_{\mathbf{x}_1^n, \mathbf{y}_1^n, \tilde{\mathbf{s}}_0^n} p_{\tilde{\mathbf{s}}_0}(\tilde{\mathbf{s}}_0) \cdot \prod_{\ell=1}^n \left(p_X(x_\ell) \cdot W(\tilde{s}_\ell, y_\ell | \tilde{s}_{\ell-1}, x_\ell) \right) \\ &= \sum_{\mathbf{x}_1^{n-1}, \mathbf{y}_1^{n-1}, \tilde{\mathbf{s}}_0^{n-1}} p_{\tilde{\mathbf{s}}_0}(\tilde{\mathbf{s}}_0) \cdot \prod_{\ell=1}^{n-1} \left(p_X(x_\ell) \cdot W(\tilde{s}_\ell, y_\ell | \tilde{s}_{\ell-1}, x_\ell) \right) \\ & \quad \cdot \underbrace{\sum_{x_n} p_X(x_n) \cdot \sum_{y_n, \tilde{s}_n} W(\tilde{s}_n, y_n | \tilde{s}_{n-1}, x_n)}_{=1} \\ &= \sum_{\mathbf{x}_1^{n-1}, \mathbf{y}_1^{n-1}, \tilde{\mathbf{s}}_0^{n-1}} p_{\tilde{\mathbf{s}}_0}(\tilde{\mathbf{s}}_0) \cdot \prod_{\ell=1}^{n-1} \left(p_X(x_\ell) \cdot W(\tilde{s}_\ell, y_\ell | \tilde{s}_{\ell-1}, x_\ell) \right) \\ &= \dots \\ &= \sum_{\tilde{\mathbf{s}}_0} p_{\tilde{\mathbf{s}}_0}(\tilde{\mathbf{s}}_0) \\ &= 1. \end{aligned} \quad (16)$$

This computation is visualized in Fig. 11 by applying suitable closing-the-box operations to the NFG in Fig. 1.

Showing that the function $Q(\mathbf{x}_1^n)$ is a pmf over \mathbf{x}_1^n is straightforward, and showing that the function $W(\mathbf{y}_1^n | \mathbf{x}_1^n)$ is a conditional pmf over \mathbf{y}_1^n given \mathbf{x}_1^n can be done analogously to the above proof. We omit the details. \square

APPENDIX B

SUPPLEMENTARY NOTES FOR SECTION II-B

The main purpose of this appendix is to prove Lemma 2 (see below) about properties of the global function associated with a quantum channel with memory as in Fig. 2. Connections to expressions involving more standard quantum information processing notation will be discussed in Appendix C.

Let $g(\mathbf{x}_1^n, \mathbf{y}_1^n, \mathbf{s}_0^n, \mathbf{s}'_0^n)$ be the global function of the NFG in Fig. 2, *i.e.*,

$$\begin{aligned} & g(\mathbf{x}_1^n, \mathbf{y}_1^n, \mathbf{s}_0^n, \mathbf{s}'_0^n) \\ & \triangleq \rho^{\mathbf{S}_0}(s_0, s'_0) \\ & \quad \cdot \prod_{\ell=1}^n \left(p_X(x_\ell) \cdot W^{(y_\ell | x_\ell)}(s_{\ell-1}, s_\ell; s'_{\ell-1}, s'_\ell) \right) \\ & \quad \cdot \delta(s'_n, s_n). \end{aligned} \quad (17)$$

Moreover, let $g(\mathbf{x}_1^n, \mathbf{y}_1^n)$ be obtained from $g(\mathbf{x}_1^n, \mathbf{y}_1^n, \mathbf{s}_0^n, \mathbf{s}'_0^n)$ by summing over \mathbf{s}_0^n and \mathbf{s}'_0^n , *i.e.*,

$$g(\mathbf{x}_1^n, \mathbf{y}_1^n) \triangleq \sum_{\mathbf{s}_0^n, \mathbf{s}'_0^n} g(\mathbf{x}_1^n, \mathbf{y}_1^n, \mathbf{s}_0^n, \mathbf{s}'_0^n), \quad (18)$$

let $Q(\mathbf{x}_1^n)$ be obtained by a suitable closing-the-box operation around parts of the NFG in Fig. 2 (see the blue box in Fig. 2), *i.e.*,

$$Q(\mathbf{x}_1^n) \triangleq \prod_{\ell=1}^n p_X(x_\ell), \quad (19)$$

and let $W(\mathbf{y}_1^n | \mathbf{x}_1^n)$ be obtained by a suitable closing-the-box operation around parts of the NFG in Fig. 2 (see the red box in Fig. 2), *i.e.*,

$$\begin{aligned} W(\mathbf{y}_1^n | \mathbf{x}_1^n) \triangleq & \sum_{s_0^n, s_0'^n} \rho^{S_0}(s_0, s_0') \\ & \cdot \prod_{\ell=1}^n \left(p_X(x_\ell) \cdot W^{(y_\ell | x_\ell)}(s_{\ell-1}, s_\ell; s_{\ell-1}', s_\ell') \right) \\ & \cdot \delta(s_n', s_n). \end{aligned} \quad (20)$$

(Note that here the closing-the-box operation for the blue box is trivial in the sense that there are no full edges completely inside the blue box, and so there are no variables to sum over.)

Lemma 2. *Assume that the channel law W is such that (9) and (10) hold. Then the function $g(\mathbf{x}_1^n, \mathbf{y}_1^n, s_0^n, s_0'^n)$ satisfies (4)–(8). Moreover, the function $Q(\mathbf{x}_1^n)$ is a pmf over \mathbf{x}_1^n , and the function $W(\mathbf{y}_1^n | \mathbf{x}_1^n)$ is a conditional pmf over \mathbf{y}_1^n given \mathbf{x}_1^n .*

Proof. We prove the first claim as follows.

- Property (4) follows immediately from (17) and the fact that all the factors appearing in this expression are complex-valued.
- Property (5) follows from (17) and the assumption that $W^{(y_\ell | x_\ell)}$ is a p.s.d. matrix for all y_ℓ and x_ℓ , and with that a Hermitian matrix for all y_ℓ and x_ℓ , *i.e.*,

$$W^{(y_\ell | x_\ell)}(s_{\ell-1}, s_\ell; s_{\ell-1}', s_\ell') = \overline{W^{(y_\ell | x_\ell)}(s_{\ell-1}', s_\ell'; s_{\ell-1}, s_\ell)} \quad (21)$$

for all $y_\ell, x_\ell, s_{\ell-1}, s_\ell, s_{\ell-1}', s_\ell'$. Moreover, one uses the real-valuedness of the Kronecker-delta function and its symmetry in the arguments.

- Property (6) can be shown by using (10) repeatedly, see the derivation in Eq. (22) at the top of the next page. This computation is visualized in Fig. 12 by applying suitable closing-the-box operations to the NFG in Fig. 2.
- Property (7) follows immediately from proving $g(\mathbf{x}_1^n, \mathbf{y}_1^n) = g(\mathbf{x}_1^n, \mathbf{y}_1^n)$ for all \mathbf{x}_1^n and \mathbf{y}_1^n , see the derivation in Eq. (23) in the middle of the next page. There, Step (a) follows from the p.s.d. property of ρ^{S_0} and $W^{(y_\ell | x_\ell)}$, along with the real-valuedness of the Kronecker-delta function and its symmetry in the arguments. Moreover, Step (b) follows from relabeling the summation variables, *i.e.*, s_0^n becomes $s_0'^n$ and vice-versa.
- Property (8) follows immediately from (18) and (6).

Showing that the function $Q(\mathbf{x}_1^n)$ is a pmf over \mathbf{x}_1^n is straightforward, and showing that the function $W(\mathbf{y}_1^n | \mathbf{x}_1^n)$ is

a conditional pmf over \mathbf{y}_1^n given \mathbf{x}_1^n can be done analogously to the above proof. We omit the details. \square

APPENDIX C SUPPLEMENTARY NOTES FOR EXAMPLE 3

The main purpose of this appendix is to give some more details w.r.t. Example 3. We do this by first discussing quantum channels without memory and then quantum channels with memory. This appendix should also help making the transition between standard quantum information processing notation and our NFG representations.

Let us emphasize that the exact details of Example 3 are *not* important. What is important is the framework that allows us to deal with this type of channels.

A. Classical Communication over a Memoryless Quantum Channel

Alice wants to communicate some classical information to Bob. To that end, for time indices $\ell = 1, \dots, n$, they can use the following quantum channel characterized by a completely-positive trace-preserving (CPTP) map

$$\begin{aligned} \Phi_\ell : \mathcal{D}(\mathcal{H}^{A_\ell}) &\rightarrow \mathcal{D}(\mathcal{H}^{B_\ell}) \\ \rho^{A_\ell} &\mapsto \rho^{B_\ell} \end{aligned}$$

The following objects appear in this expression:

- \mathcal{H}^{A_ℓ} is a Hilbert space on Alice's side.
- \mathcal{H}^{B_ℓ} is a Hilbert space on Bob's side.
- $\mathcal{D}(\mathcal{H}^{A_\ell})$ is the set of density operators defined on \mathcal{H}^{A_ℓ} .
- $\mathcal{D}(\mathcal{H}^{B_\ell})$ is the set of density operators defined on \mathcal{H}^{B_ℓ} .

We make the following assumptions:

- All Hilbert spaces are finite dimensional.
- In order to be specific, the mapping Φ_ℓ is defined via Kraus operators $\{E_{k_\ell}\}_{k_\ell}$, *i.e.*,

$$\Phi_\ell(\rho^{A_\ell}) \triangleq \sum_{k_\ell} E_{k_\ell} \rho^{A_\ell} E_{k_\ell}^H. \quad (24)$$

Note that the operators $\{E_{k_\ell}\}_{k_\ell}$ have to satisfy the condition $\sum_{k_\ell} E_{k_\ell}^H E_{k_\ell} = I$, where I is an identity matrix of suitable size.

- Alice can prepare quantum states in \mathcal{H}^{A_ℓ} described by density operators $\{\rho_{x_\ell}^A\}_{x_\ell \in \mathcal{X}}$.
- Bob can make a quantum measurement on $\mathcal{D}(\mathcal{H}^{B_\ell})$ described by the measurement operators $\{M_{y_\ell}\}_{y_\ell \in \mathcal{Y}}$. Specifically, for $\rho^{B_\ell} \in \mathcal{D}(\mathcal{H}^{B_\ell})$, the measurement outcome is $y_\ell \in \mathcal{Y}$ with probability

$$p_{Y_\ell}(y_\ell) = \text{Tr}(M_{y_\ell} \rho^{B_\ell} M_{y_\ell}^H). \quad (25)$$

Note that the operators $\{M_{y_\ell}\}_{y_\ell \in \mathcal{Y}}$ have to satisfy the condition $\sum_{y_\ell} M_{y_\ell}^H M_{y_\ell} = I$.

For further details about CPTP maps and measurement operators, see, *e.g.*, [12].

Alice and Bob use n independent instantiations of this channel to transmit classical information as follows.

$$\begin{aligned}
\sum_{\mathbf{x}_1^n, \mathbf{y}_1^n, \mathbf{s}_0^n, \mathbf{s}'_0^n} g(\mathbf{x}_1^n, \mathbf{y}_1^n, \mathbf{s}_0^n, \mathbf{s}'_0^n) &= \sum_{\mathbf{x}_1^n, \mathbf{y}_1^n, \mathbf{s}_0^n, \mathbf{s}'_0^n} \rho^{\mathbf{S}_0}(s_0, s'_0) \cdot \prod_{\ell=1}^n \left(p_X(x_\ell) \cdot W^{(y_\ell|x_\ell)}(s_{\ell-1}, s_\ell; s'_{\ell-1}, s'_\ell) \right) \cdot \delta(s'_n, s_n) \\
&= \sum_{\mathbf{x}_1^{n-1}, \mathbf{y}_1^{n-1}, \mathbf{s}_0^{n-1}, \mathbf{s}'_0^{n-1}} \rho^{\mathbf{S}_0}(s_0, s'_0) \cdot \prod_{\ell=1}^{n-1} \left(p_X(x_\ell) \cdot W^{(y_\ell|x_\ell)}(s_{\ell-1}, s_\ell; s'_{\ell-1}, s'_\ell) \right) \\
&\quad \cdot \underbrace{\sum_{x_n} p_X(x_n) \cdot \sum_{y_n, s_n, s'_n} W^{(y_n|x_n)}(s_{n-1}, s_n; s'_{n-1}, s'_n) \cdot \delta(s'_n, s_n)}_{= \delta(s'_{n-1}, s_{n-1})} \\
&\quad \underbrace{\hspace{10em}}_{= \delta(s'_{n-1}, s_{n-1})} \\
&= \sum_{\mathbf{x}_1^{n-1}, \mathbf{y}_1^{n-1}, \mathbf{s}_0^{n-1}, \mathbf{s}'_0^{n-1}} \rho^{\mathbf{S}_0}(s_0, s'_0) \cdot \prod_{\ell=1}^{n-1} \left(p_X(x_\ell) \cdot W^{(y_\ell|x_\ell)}(s_{\ell-1}, s_\ell; s'_{\ell-1}, s'_\ell) \right) \cdot \delta(s'_{n-1}, s_{n-1}) \\
&= \dots \\
&= \sum_{s_0, s'_0} \rho^{\mathbf{S}_0}(s_0, s'_0) \cdot \delta(s'_0, s_0) \\
&= 1 .
\end{aligned} \tag{22}$$

$$\begin{aligned}
\overline{g(\mathbf{x}_1^n, \mathbf{y}_1^n)} &= \overline{\sum_{\mathbf{s}_0^n, \mathbf{s}'_0^n} g(\mathbf{x}_1^n, \mathbf{y}_1^n, \mathbf{s}_0^n, \mathbf{s}'_0^n)} \\
&= \overline{\sum_{\mathbf{s}_0^n, \mathbf{s}'_0^n} \rho^{\mathbf{S}_0}(s_0, s'_0) \cdot \prod_{\ell=1}^n \left(p_X(x_\ell) \cdot W^{(y_\ell|x_\ell)}(s_{\ell-1}, s_\ell; s'_{\ell-1}, s'_\ell) \right) \cdot \delta(s'_n, s_n)} \\
&= \sum_{\mathbf{s}_0^n, \mathbf{s}'_0^n} \overline{\rho^{\mathbf{S}_0}(s_0, s'_0)} \cdot \prod_{\ell=1}^n \left(\overline{p_X(x_\ell)} \cdot \overline{W^{(y_\ell|x_\ell)}(s_{\ell-1}, s_\ell; s'_{\ell-1}, s'_\ell)} \right) \cdot \overline{\delta(s'_n, s_n)} \\
&\stackrel{(a)}{=} \sum_{\mathbf{s}_0^n, \mathbf{s}'_0^n} \rho^{\mathbf{S}_0}(s'_0, s_0) \cdot \prod_{\ell=1}^n \left(p_X(x_\ell) \cdot W^{(y_\ell|x_\ell)}(s'_{\ell-1}, s'_\ell; s_{\ell-1}, s_\ell) \right) \cdot \delta(s_n, s'_n) \\
&\stackrel{(b)}{=} \sum_{\mathbf{s}_0^n, \mathbf{s}'_0^n} \rho^{\mathbf{S}_0}(s_0, s'_0) \cdot \prod_{\ell=1}^n \left(p_X(x_\ell) \cdot W^{(y_\ell|x_\ell)}(s_{\ell-1}, s_\ell; s'_{\ell-1}, s'_\ell) \right) \cdot \delta(s'_n, s_n) \\
&= g(\mathbf{x}_1^n, \mathbf{y}_1^n) .
\end{aligned} \tag{23}$$

- Alice uses a classical code to encode her information word $\mathbf{u} = (u_1, u_2, \dots, u_k) \in \mathcal{U}^k$ into a codeword $\mathbf{x} = (x_1, x_2, \dots, x_n) \in \mathcal{X}^n$.
- At time instance ℓ , Alice transmits $\rho^{\mathbf{A}_\ell} = \rho_{x_\ell}^{\mathbf{A}}$ via the ℓ -th instantiation of the memoryless quantum channel to Bob.
- Bob makes a quantum measurement on $\rho^{\mathbf{B}_\ell} \triangleq \Phi_\ell(\rho^{\mathbf{A}_\ell})$ described by the measurement operators $\{M_{y_\ell}\}_{y_\ell \in \mathcal{Y}}$. The measurement outcome is called y_ℓ .
- Bob decodes $\mathbf{y} = (y_1, y_2, \dots, y_n) \in \mathcal{Y}^n$ toward obtaining an estimate $\hat{\mathbf{u}}$ of \mathbf{u} .

probability of y_ℓ given x_ℓ . We obtain

$$\begin{aligned}
W(y_\ell|x_\ell) &= \text{Tr} \left(M_{y_\ell} \left(\sum_{k_\ell} E_{k_\ell} \rho_{x_\ell}^{\mathbf{A}} E_{k_\ell}^{\mathbf{H}} \right) M_{y_\ell}^{\mathbf{H}} \right) \\
&= \sum_{k_\ell} \text{Tr} \left(M_{y_\ell} E_{k_\ell} \rho_{x_\ell}^{\mathbf{A}} E_{k_\ell}^{\mathbf{H}} M_{y_\ell}^{\mathbf{H}} \right) .
\end{aligned} \tag{26}$$

We emphasize that in our setup, the operators $\{\rho_{x_\ell}^{\mathbf{A}}\}_{x_\ell \in \mathcal{X}}$ and $\{M_{y_\ell}\}_{y_\ell \in \mathcal{Y}}$ are given, *i.e.*, they cannot be chosen by Alice and Bob, respectively.

Let $W(y_\ell|x_\ell) = p_{Y_\ell|X_\ell}(y_\ell|x_\ell)$ be the channel law, *i.e.*, the

Introducing suitable orthonormal bases to express the opera-

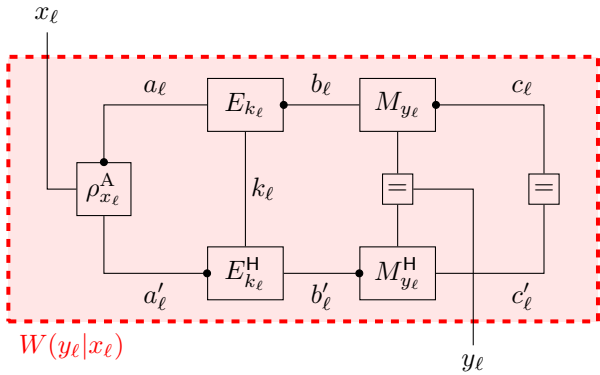


Fig. 9. Classical communication over a memoryless quantum channel.

tors, we can write this as

$$\begin{aligned}
 W(y_\ell|x_\ell) &= \sum_{k_\ell} \sum_{a_\ell, a'_\ell} \sum_{b_\ell, b'_\ell} \sum_{c_\ell, c'_\ell} M_{y_\ell}(c_\ell, b_\ell) \cdot E_{k_\ell}(b_\ell, a_\ell) \\
 &\quad \cdot \rho_{x_\ell}^A(a_\ell, a'_\ell) \cdot E_{k_\ell}^H(a'_\ell, b'_\ell) \cdot M_{y_\ell}^H(b'_\ell, c'_\ell) \cdot \delta(c'_\ell, c_\ell). \quad (27)
 \end{aligned}$$

These calculations can be visualized with the help of the NFG in Fig. 9. Namely, the global function is

$$\begin{aligned}
 g(x_\ell, y_\ell, k_\ell, a_\ell, a'_\ell, b_\ell, b'_\ell, c_\ell, c'_\ell) &= M_{y_\ell}(c_\ell, b_\ell) \cdot E_{k_\ell}(b_\ell, a_\ell) \cdot \rho_{x_\ell}^A(a_\ell, a'_\ell) \\
 &\quad \cdot E_{k_\ell}^H(a'_\ell, b'_\ell) \cdot M_{y_\ell}^H(b'_\ell, c'_\ell) \cdot \delta(c'_\ell, c_\ell), \quad (28)
 \end{aligned}$$

and the above-mentioned function $W(y_\ell|x_\ell)$ is obtained by a suitably closing-the-box operation (see the red box in Fig. 9), where we sum over all variables associated with edges that are completely inside the box.

Finally, note that the channel law of n independent instantiations of this channel is given by

$$W(\mathbf{y}_1^n | \mathbf{x}_1^n) = \prod_{\ell=1}^n W(y_\ell | x_\ell). \quad (29)$$

B. Classical Communication over a Quantum Channel with Memory

Having discussed quantum channels without memory, we now turn our attention to quantum channels with memory. Alice wants again to communicate some classical information to Bob. For time indices $\ell = 1, \dots, n$, they can use the following quantum channel characterized by a CPTP map

$$\begin{aligned}
 \Phi_\ell : \mathcal{D}(\mathcal{H}^{A_\ell} \otimes \mathcal{H}^{S_{\ell-1}}) &\rightarrow \mathcal{D}(\mathcal{H}^{B_\ell} \otimes \mathcal{H}^{S_\ell}) \\
 \rho^{A_\ell S_{\ell-1}} &\mapsto \rho^{B_\ell S_\ell}
 \end{aligned}$$

The following objects appear in this expression:

- \mathcal{H}^{A_ℓ} is a Hilbert space on Alice's side.
- \mathcal{H}^{B_ℓ} is a Hilbert space on Bob's side.
- $\mathcal{H}^{S_{\ell-1}}$ is the Hilbert space relevant for the memory of the channel at time index $\ell - 1$.

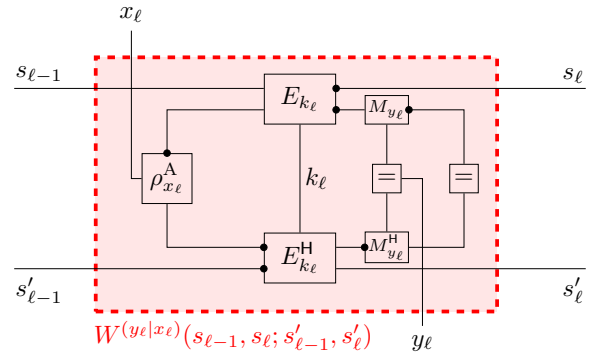


Fig. 10. Classical communication over a quantum channel with memory: internal details of $W(y_\ell|x_\ell)(s_{\ell-1}, s_\ell; s'_{\ell-1}, s'_\ell)$ in (36).

- \mathcal{H}^{S_ℓ} is the Hilbert space relevant for the memory of the channel at time index ℓ .
- $\mathcal{D}(\mathcal{H}^{A_\ell} \otimes \mathcal{H}^{S_{\ell-1}})$ is the set of density operators defined on $\mathcal{H}^{A_\ell} \otimes \mathcal{H}^{S_{\ell-1}}$.
- $\mathcal{D}(\mathcal{H}^{B_\ell} \otimes \mathcal{H}^{S_\ell})$ is the set of density operators defined on $\mathcal{H}^{B_\ell} \otimes \mathcal{H}^{S_\ell}$.

We make the following assumptions:

- All Hilbert spaces are finite dimensional.
- In order to be specific, the mapping Φ_ℓ is defined via Kraus operators $\{E_{k_\ell}\}_{k_\ell}$, i.e.,

$$\Phi_\ell(\rho^{A_\ell S_{\ell-1}}) \triangleq \sum_{k_\ell} E_{k_\ell} \rho^{A_\ell S_{\ell-1}} E_{k_\ell}^H. \quad (30)$$

Note that the operators $\{E_{k_\ell}\}_{k_\ell}$ have to satisfy the condition $\sum_{k_\ell} E_{k_\ell} E_{k_\ell}^H = I$.

- Alice can prepare quantum states in \mathcal{H}^{A_ℓ} described by density operators $\{\rho_{x_\ell}^A\}_{x_\ell \in \mathcal{X}}$. We assume that, given x_ℓ , what Alice does is independent of the state of the channel at time index $\ell - 1$, i.e., $\rho^{A_\ell S_{\ell-1}} = \rho_{x_\ell}^A \otimes \rho^{S_{\ell-1}}$.
- Bob can make a quantum measurement on $\mathcal{D}(\mathcal{H}^{B_\ell})$ described by the measurement operators $\{M_{y_\ell}\}_{y_\ell \in \mathcal{Y}}$. Specifically, for $\rho^{B_\ell} \in \mathcal{D}(\mathcal{H}^{B_\ell})$, the measurement outcome is $y_\ell \in \mathcal{Y}$ with probability

$$p_{Y_\ell}(y_\ell) = \text{Tr}(M_{y_\ell} \rho^{B_\ell} M_{y_\ell}^H). \quad (31)$$

Note that the operators $\{M_{y_\ell}\}_{y_\ell \in \mathcal{Y}}$ have to satisfy the condition $\sum_{y_\ell} M_{y_\ell}^H M_{y_\ell} = I$.

For further details about quantum channels with memory we refer to the survey papers by Kretschmann and Werner [13] and by Caruso *et al.* [14].

Alice and Bob use n instantiations of this channel to transmit classical information as follows:

- Alice uses a classical code to encode her information word $\mathbf{u} = (u_1, u_2, \dots, u_k) \in \mathcal{U}^k$ into a codeword $\mathbf{x} = (x_1, x_2, \dots, x_n) \in \mathcal{X}^n$.
- At time instance ℓ , Alice transmits $\rho^{A_\ell} = \rho_{x_\ell}^A$ via the ℓ -th instantiation of the quantum channel to Bob.
- Bob makes a quantum measurement on

$$\rho^{B_\ell} \triangleq \text{Tr}_{S_\ell}(\rho^{B_\ell S_\ell}) \triangleq \text{Tr}_{S_\ell}(\Phi_\ell(\rho^{A_\ell S_{\ell-1}})) \quad (32)$$

described by the measurement operators $\{M_{y_\ell}\}_{y_\ell \in \mathcal{Y}}$. The measurement outcome is called y_ℓ .

- Bob decodes $\mathbf{y} = (y_1, y_2, \dots, y_n) \in \mathcal{Y}^n$ toward obtaining an estimate $\hat{\mathbf{u}}$ of \mathbf{u} .

We emphasize that in our setup, the operators $\{\rho_{x_\ell}^A\}_{x_\ell \in \mathcal{X}}$ and $\{M_{y_\ell}\}_{y_\ell \in \mathcal{Y}}$ are given, *i.e.*, they cannot be chosen by Alice and Bob, respectively.

With this, the probability of receiving y_ℓ , given that x_ℓ was sent and given that the channel state at time $\ell - 1$ is known to be $\rho^{S_{\ell-1}}$, equals⁴

$$\text{Tr} \left(M_{y_\ell} \text{Tr}_{S_\ell} \left(\sum_{k_\ell} E_{k_\ell} (\rho_{x_\ell}^A \otimes \rho^{S_{\ell-1}}) E_{k_\ell}^H \right) M_{y_\ell}^H \right), \quad (33)$$

which can also be written as

$$\text{Tr} \left((M_{y_\ell} \otimes I^{S_\ell}) \left(\sum_{k_\ell} E_{k_\ell} (\rho_{x_\ell}^A \otimes \rho^{S_{\ell-1}}) E_{k_\ell}^H \right) (M_{y_\ell}^H \otimes I^{S_\ell}) \right). \quad (34)$$

Moreover, assuming that x_ℓ was sent, that y_ℓ was observed, and that the channel state at time $\ell - 1$ is known to be $\rho^{S_{\ell-1}}$, the channel state at time index ℓ is given by

$$\frac{\text{Tr}_{B_\ell} \left((M_{y_\ell} \otimes I^{S_\ell}) \left(\sum_{k_\ell} E_{k_\ell} (\rho_{x_\ell}^A \otimes \rho^{S_{\ell-1}}) E_{k_\ell}^H \right) (M_{y_\ell}^H \otimes I^{S_\ell}) \right)}{\text{Tr} \left((M_{y_\ell} \otimes I^{S_\ell}) \left(\sum_{k_\ell} E_{k_\ell} (\rho_{x_\ell}^A \otimes \rho^{S_{\ell-1}}) E_{k_\ell}^H \right) (M_{y_\ell}^H \otimes I^{S_\ell}) \right)}. \quad (35)$$

Note that the denominator in (35) equals the expressions in (33) and (34).

In order to obtain an NFG representation of the setup in this section, we introduce

$$\begin{aligned} & W^{(y_\ell|x_\ell)}(s_{\ell-1}, s_\ell; s'_{\ell-1}, s'_\ell) \\ & \triangleq \sum_{k_\ell} \sum_{a_\ell, a'_\ell} \sum_{b_\ell, b'_\ell} \sum_{c_\ell, c'_\ell} M_{y_\ell}(c_\ell, b_\ell) \cdot E_{k_\ell}((b_\ell, s_\ell), (a_\ell, s_{\ell-1})) \\ & \quad \cdot \rho_{x_\ell}^A(a_\ell, a'_\ell) \cdot E_{k_\ell}^H((a'_\ell, s'_{\ell-1}), (b'_\ell, s'_\ell)) \cdot M_{y_\ell}^H(b'_\ell, c'_\ell) \\ & \quad \cdot \delta(c'_\ell, c_\ell). \end{aligned} \quad (36)$$

Note that this function is obtained by a suitably closing-the-box operation (see the red box in Fig. 10), where we sum over all variables associated with edges that are completely inside the box. (Note that the edge labels inside the box are analogous to the edge labels in Fig. 9. However, for simplicity, we have omitted most of them.)

On the side, we note that the corresponding NFG for the Quantum Gilbert–Elliott Channel in Fig. 4 contains additional U -boxes representing a unitary evolution of the channel state. By redefining E_{k_ℓ} to $(I^{B_\ell} \otimes U) E_{k_\ell}$, the NFG in Fig. 4 could be brought into the form of the NFG in Fig. 10.⁵

With the function $W^{(y_\ell|x_\ell)}(s_{\ell-1}, s_\ell; s'_{\ell-1}, s'_\ell)$ in hand, along with the corresponding (partial) NFG in Fig. 10, we can define an NFG for the overall setup as in Fig. 2.

⁴Note that what $\rho^{S_{\ell-1}}$ is, depends on the knowledge/ignorance of components of $\mathbf{x}_1^{\ell-1}$ and $\mathbf{y}_1^{\ell-1}$. For an example, see later parts of this appendix.

⁵Observe that the redefined E_{k_ℓ} still satisfies $\sum_{k_\ell} E_{k_\ell}^H E_{k_\ell} = I$.

Note that the boxes labeled W represent the function $W^{(y_\ell|x_\ell)}(s_{\ell-1}, s_\ell; s'_{\ell-1}, s'_\ell)$ for $\ell = 1, \dots, n$. Because the function $W^{(y_\ell|x_\ell)}(s_{\ell-1}, s_\ell; s'_{\ell-1}, s'_\ell)$ satisfies (9) and (10), the global function g of the NFG in Fig. 2 satisfies (4)–(8). (See Appendix B for details.)

All probabilities and density operators of interest can be obtained by suitably summing over variables of the global function of the NFG in Fig. 2. For example, for fixed $\mathbf{y}_1^{\ell-1} = \check{\mathbf{y}}_1^{\ell-1}$ and $x_\ell = \check{x}_\ell$, the probability $p_{Y_\ell|X_\ell, \mathbf{Y}_1^{\ell-1}}(y_\ell|\check{x}_\ell, \check{\mathbf{y}}_1^{\ell-1})$ can be obtained as follows:

$$\begin{aligned} & p_{Y_\ell|X_\ell, \mathbf{Y}_1^{\ell-1}}(y_\ell|\check{x}_\ell, \check{\mathbf{y}}_1^{\ell-1}) \\ & \propto p_{X_\ell, \mathbf{Y}_1^{\ell-1}, Y_\ell}(\check{x}_\ell, \check{\mathbf{y}}_1^{\ell-1}, y_\ell) \\ & = \sum_{\mathbf{x}_1^{\ell-1}, \mathbf{x}_{\ell+1}^n, \mathbf{y}_{\ell+1}^n, \mathbf{s}_0^n, \mathbf{s}'_0^n} g(\mathbf{x}_1^{\ell-1}, \check{x}_\ell, \mathbf{x}_{\ell+1}^n, \check{\mathbf{y}}_1^{\ell-1}, \mathbf{y}_\ell^n, \mathbf{s}_0^n, \mathbf{s}'_0^n). \end{aligned} \quad (37)$$

Here, the proportionality constant is chosen such that the left-hand side is a valid conditional pmf. The computation of this function via closing-the-box operations is visualized in Fig. 14. Some comments:

- Applying the closing-the-box operation to the magenta box results in the function $\sigma_{|\check{\mathbf{y}}_1^{\ell-1}}^{S_{\ell-1}}(s_{\ell-1}, s'_{\ell-1})$.⁶
- Applying the closing-the-box operation to the green box results in the function $\delta(s'_\ell, s_\ell)$, *i.e.*, a degree-2 equality function node.
- Applying the closing-the-box operation to the yellow box results in the function $p_{X_\ell, \mathbf{Y}_1^{\ell-1}, Y_\ell}(\check{x}_\ell, \check{\mathbf{y}}_1^{\ell-1}, y_\ell)$, from which the desired function $p_{Y_\ell|X_\ell, \mathbf{Y}_1^{\ell-1}}(y_\ell|\check{x}_\ell, \check{\mathbf{y}}_1^{\ell-1})$ can be easily obtained by normalization.

Note that, mathematically, applying the closing-the-box operation to the yellow box gives the following function (with argument y_ℓ)

$$\begin{aligned} & \sum_{s_{\ell-1}, s'_{\ell-1}, s_\ell, s'_\ell} \sigma_{|\check{\mathbf{y}}_1^{\ell-1}}^{S_{\ell-1}}(s_{\ell-1}, s'_{\ell-1}) \cdot p_X(\check{x}_\ell) \\ & \quad \cdot W^{(y_\ell|\check{x}_\ell)}(s_{\ell-1}, s_\ell; s'_{\ell-1}, s'_\ell) \cdot \delta(s'_\ell, s_\ell). \end{aligned} \quad (38)$$

- If $\rho^{S_{\ell-1}} = \sigma_{|\check{\mathbf{y}}_1^{\ell-1}}^{S_{\ell-1}}$, then the expressions in (33) and (34) equal $p_{Y_\ell|X_\ell, \mathbf{Y}_1^{\ell-1}}(y_\ell|\check{x}_\ell, \check{\mathbf{y}}_1^{\ell-1})$. This connection between the NFG approach and the standard quantum information processing notation can be established by inserting (36) into (38).
- Functions like $\sigma_{|\check{\mathbf{y}}_1^{\ell-1}}^{S_{\ell-1}}$ can be computed efficiently by recursive computations. For more details, see Appendix D.
- The analogous NFG for the classical setup is shown in Fig. 13.

Let us also point out that, very often, the desired functions and quantities are based on the same partial results. The NFG framework is very helpful to visualize these partial results and

⁶The subscript “ $|\check{\mathbf{y}}_1^{\ell-1}$ ” emphasizes that $\sigma_{|\check{\mathbf{y}}_1^{\ell-1}}^{S_{\ell-1}}(s_{\ell-1}, s'_{\ell-1})$ is based on the knowledge of $\mathbf{y}_1^{\ell-1} = \check{\mathbf{y}}_1^{\ell-1}$.

to show how these partial results are combined to obtain the desired functions and quantities.

APPENDIX D

SUPPLEMENTARY NOTES FOR SECTION III

In this appendix, we first present a brief summary of the approach for estimating the information rate of FSMCs as developed in [4], and then extend this method to quantum channels with memory.

A. Estimation of $I(\mathbf{X}; \mathbf{Y})$ for Classical Channels with Memory

We make the following assumptions.

- As already mentioned, the derivations in this paper are for the case where the input process $\mathbf{X} = (X_1, X_2, \dots)$ is an i.i.d. process. The results can be generalized to other stationary ergodic input processes that can be represented by a finite-state-machine source (FSMS). Technically, this is done by defining a new state that combines the FSMS state and the FSMC state.
- We assume that the FSMC is indecomposable, which roughly means that in the long term the behavior of the channel is independent of the initial channel state distribution $p_{\tilde{s}_0}$ (see [1] for the exact definition). For such channels and stationary ergodic input processes, the information rate $I(\mathbf{X}; \mathbf{Y})$ is well defined.

Definition 3. The information rate is defined to be

$$I(\mathbf{X}; \mathbf{Y}) \triangleq \lim_{n \rightarrow \infty} \frac{1}{n} I(X_1, \dots, X_n; Y_1, \dots, Y_n). \quad (39)$$

Equivalently, it can be defined as

$$I(\mathbf{X}; \mathbf{Y}) = H(\mathbf{X}) + H(\mathbf{Y}) - H(\mathbf{X}, \mathbf{Y}), \quad (40)$$

where

$$H(\mathbf{X}) = \lim_{n \rightarrow \infty} \frac{1}{n} H(\mathbf{X}_1^n),$$

$$H(\mathbf{Y}) = \lim_{n \rightarrow \infty} \frac{1}{n} H(\mathbf{Y}_1^n),$$

$$H(\mathbf{X}, \mathbf{Y}) = \lim_{n \rightarrow \infty} \frac{1}{n} H(\mathbf{X}_1^n, \mathbf{Y}_1^n).$$

■

We proceed as in [4]. (For more background information, see the references in [4], in particular [22].) Namely, because of (40) and because

$$-\frac{1}{n} \log p(\mathbf{X}_1^n) \rightarrow H(\mathbf{X}) \quad \text{w.p. 1}, \quad (41)$$

$$-\frac{1}{n} \log p(\mathbf{Y}_1^n) \rightarrow H(\mathbf{Y}) \quad \text{w.p. 1}, \quad (42)$$

$$-\frac{1}{n} \log p(\mathbf{X}_1^n, \mathbf{Y}_1^n) \rightarrow H(\mathbf{X}, \mathbf{Y}) \quad \text{w.p. 1}, \quad (43)$$

we can choose some finite positive integer n and approximate $I(\mathbf{X}; \mathbf{Y})$ as follows

$$I(\mathbf{X}; \mathbf{Y}) \approx \hat{I}(\mathbf{X}; \mathbf{Y}), \quad (44)$$

where

$$\hat{I}(\mathbf{X}; \mathbf{Y}) \triangleq -\frac{1}{n} \log p(\tilde{\mathbf{x}}_1^n) - \frac{1}{n} \log p(\tilde{\mathbf{y}}_1^n) + \frac{1}{n} \log p(\tilde{\mathbf{x}}_1^n, \tilde{\mathbf{y}}_1^n) \quad (45)$$

and where $\tilde{\mathbf{x}}_1^n$ and $\tilde{\mathbf{y}}_1^n$ are some input and output sequences, respectively, randomly generated according to

$$p_{\mathbf{X}_1^n, \mathbf{Y}_1^n}(\mathbf{x}_1^n, \mathbf{y}_1^n) = \sum_{\tilde{s}_0^n} p_{\tilde{s}_0}(\tilde{s}_0) \cdot Q(\mathbf{x}_1^n) \cdot W(\mathbf{y}_1^n, \tilde{s}_1^n | \mathbf{x}_1^n, \tilde{s}_0). \quad (46)$$

Note that $\tilde{\mathbf{x}}$ can be obtained by simulating the input process and $\tilde{\mathbf{y}}$ can be obtained by simulating the channel for the given input process realization $\tilde{\mathbf{x}}$.

We continue by showing how the three terms appearing on the right-hand side of (45) can be computed efficiently. We show it explicitly for the second term, and then outline it for the first and the third term.

In order to efficiently compute the second term on the right-hand side of (45), i.e., $-\frac{1}{n} \log p(\mathbf{Y}_1^n)$, we consider the *state metric* defined in [4] as

$$\mu_\ell^{\mathbf{Y}}(\tilde{s}_\ell) \triangleq \sum_{\mathbf{x}_1^\ell} \sum_{\tilde{s}_0^{\ell-1}} p_{\tilde{s}_0}(\tilde{s}_0) \cdot Q(\mathbf{x}_1^\ell) \cdot W(\tilde{\mathbf{y}}_1^\ell, \tilde{s}_1^\ell | \mathbf{x}_1^\ell, \tilde{s}_0). \quad (47)$$

Note that

$$p_{\mathbf{Y}_1^n}(\tilde{\mathbf{y}}_1^n) = \sum_{\tilde{s}_n} \mu_n^{\mathbf{Y}}(\tilde{s}_n) \quad (48)$$

and that $\mu_\ell^{\mathbf{Y}}(\tilde{s}_\ell)$ can be calculated recursively via

$$\begin{aligned} \mu_\ell^{\mathbf{Y}}(\tilde{s}_\ell) &= \sum_{x_\ell} \sum_{\tilde{s}_{\ell-1}} \mu_{\ell-1}^{\mathbf{Y}}(\tilde{s}_{\ell-1}) \cdot Q(x_\ell | \mathbf{x}_1^{\ell-1}) \cdot W(\tilde{s}_\ell, \tilde{y}_\ell | \tilde{s}_{\ell-1}, x_\ell) \\ &= \sum_{x_\ell} \sum_{\tilde{s}_{\ell-1}} \mu_{\ell-1}^{\mathbf{Y}}(\tilde{s}_{\ell-1}) \cdot p_X(x_\ell) \cdot W(\tilde{s}_\ell, \tilde{y}_\ell | \tilde{s}_{\ell-1}, x_\ell). \end{aligned} \quad (49)$$

These definitions are visualized in Fig. 15 by applying suitable closing-the-box operations to the NFG in Fig. 1.

However, since the value of $\mu_\ell^{\mathbf{Y}}(\tilde{s}_\ell)$ tends to zero as ℓ grows, such recursive calculations are numerically unstable. A solution is to *normalize* $\mu_\ell^{\mathbf{Y}}(\tilde{s}_\ell)$ during such recursive calculations and to keep track of the scaling coefficients. Namely,

$$\bar{\mu}_\ell^{\mathbf{Y}}(\tilde{s}_\ell) \triangleq \lambda_\ell^{\mathbf{Y}} \cdot \sum_{x_\ell} \sum_{\tilde{s}_{\ell-1}} \mu_{\ell-1}^{\mathbf{Y}}(\tilde{s}_{\ell-1}) \cdot p_X(x_\ell) \cdot W(\tilde{s}_\ell, \tilde{y}_\ell | \tilde{s}_{\ell-1}, x_\ell), \quad (50)$$

where the scaling factor $\lambda_\ell^{\mathbf{Y}} > 0$ is defined such that $\sum_{\tilde{s}_\ell} \bar{\mu}_\ell^{\mathbf{Y}}(\tilde{s}_\ell) = 1$. With this, Eq. (48) can be rewritten as

$$p_{\mathbf{Y}_1^n}(\tilde{\mathbf{y}}_1^n) = \prod_{\ell=1}^n (\lambda_\ell^{\mathbf{Y}})^{-1}. \quad (51)$$

Finally, we arrive at the following efficient procedure for computing $-\frac{1}{n} \log p(\tilde{\mathbf{y}}_1^n)$:

- Replace (46) by

$$p_{\mathbf{X}_1^n, \mathbf{Y}_1^n}(\mathbf{x}_1^n, \mathbf{y}_1^n) = \sum_{\mathbf{s}_0^n, \mathbf{s}'_0^n} \rho^{S_0}(s_0, s'_0) \cdot Q(\mathbf{x}_1^n) \cdot \prod_{\ell=1}^n \left(W^{(y_\ell|x_\ell)}(s_{\ell-1}, s_\ell; s'_{\ell-1}, s'_\ell) \right) \cdot \delta(s'_n, s_n). \quad (54)$$

- Replace the state metric μ_ℓ^Y in (47) by the *state operator* σ_ℓ^Y , where

$$\sigma_\ell^Y(s_\ell, s'_\ell) \triangleq \sum_{\mathbf{x}_1^\ell, \mathbf{s}_0^{\ell-1}, \mathbf{s}'_0^{\ell-1}} \rho^{S_0}(s_0, s'_0) \cdot Q(\mathbf{x}_1^\ell) \cdot \prod_{h=1}^{\ell} W^{(\tilde{y}_h|\tilde{x}_h)}(s_{h-1}, s_h; s'_{h-1}, s'_h). \quad (55)$$

- Replace (48) by

$$p_{\mathbf{Y}_1^n}(\mathbf{y}_1^n) = \sum_{s_n, s'_n} \sigma_n^Y(s_n, s'_n) \cdot \delta(s'_n, s_n). \quad (56)$$

- Replace (49) by

$$\sigma_\ell^Y(s_\ell, s'_\ell) \triangleq \sum_{x_\ell} \sum_{s_{\ell-1}, s'_{\ell-1}} \sigma_{\ell-1}^Y(s_{\ell-1}, s'_{\ell-1}) \cdot p_X(x_\ell) \cdot W^{(\tilde{y}_\ell|x_\ell)}(s_{\ell-1}, s_\ell; s'_{\ell-1}, s'_\ell). \quad (57)$$

- Replace (50) by

$$\bar{\sigma}_\ell^Y(s_\ell, s'_\ell) \triangleq \lambda_\ell^Y \cdot \sum_{x_\ell} \sum_{s_{\ell-1}, s'_{\ell-1}} \sigma_{\ell-1}^Y(s_{\ell-1}, s'_{\ell-1}) \cdot p_X(x_\ell) \cdot W^{(\tilde{y}_\ell|x_\ell)}(s_{\ell-1}, s_\ell; s'_{\ell-1}, s'_\ell), \quad (58)$$

where the scaling factor $\lambda_\ell^Y > 0$ is defined such that $\sum_{s_\ell, s'_\ell} \sigma_\ell^Y(s_\ell, s'_\ell) \cdot \delta(s'_n, s_n) = 1$, i.e., $\text{tr}(\bar{\sigma}_\ell^Y) = 1$.

- Replace the state metric $\mu_\ell^{X,Y}$ in (53) by the *state operator* $\sigma_\ell^{X,Y}$, where

$$\sigma_\ell^{X,Y}(s_\ell, s'_\ell) \triangleq \sum_{\mathbf{s}_0^{\ell-1}, \mathbf{s}'_0^{\ell-1}} \rho^{S_0}(s_0, s'_0) \cdot Q(\tilde{\mathbf{x}}_1^\ell) \cdot \prod_{h=1}^{\ell} W^{(\tilde{y}_h|\tilde{x}_h)}(s_{h-1}, s_h; s'_{h-1}, s'_h). \quad (59)$$

- For $\ell = 1, \dots, n$, iteratively compute the normalized state metric and with that the scaling factors λ_ℓ^Y .
- Conclude with the result

$$-\frac{1}{n} \log p_{\mathbf{Y}_1^n}(\mathbf{y}_1^n) = \frac{1}{n} \sum_{\ell=1}^n \log(\lambda_\ell^Y). \quad (52)$$

The third term on the right-hand side of (45) can be evaluated by an analogous procedure, where the state metric $\mu_\ell^Y(\tilde{s}_\ell)$ is replaced by the state metric

$$\mu_\ell^{X,Y}(\tilde{s}_\ell) \triangleq \sum_{\tilde{\mathbf{s}}_0^{\ell-1}} p_{\tilde{\mathbf{s}}_0}(\tilde{\mathbf{s}}_0) \cdot Q(\tilde{\mathbf{x}}_1^\ell) \cdot W(\tilde{\mathbf{y}}_1^\ell, \tilde{\mathbf{s}}_1^\ell | \tilde{\mathbf{x}}_1^\ell). \quad (53)$$

The iterative calculation of $\mu_\ell^{X,Y}(\tilde{s}_\ell)$ is visualized in Fig. 17 by applying suitable closing-the-box operations to the NFG in Fig. 1.

Finally, the first term on the right-hand side of (45) can be trivially evaluated if X is an i.i.d. process, and with a similar approach as above if it is described by a finite-state process.

B. Estimation of $I(X; Y)$ for Quantum Channels with Memory

The development in this section is very similar to the development in Section D-A. This similarity stems from the similarity of Figs. 1 and 2, and highlights one of the benefits of the factor-graph approach that we take to estimate information rates of quantum channels with memory.

We make the following assumptions.

- As already mentioned, the derivations in this paper are for the case where the input process $X = (X_1, X_2, \dots)$ is an i.i.d. process. The results can be generalized to other stationary ergodic input processes that can be represented by a finite-state-machine source (FSMS). Technically, this is done by defining a new state that combines the FSMS state and the channel state.
- We assume that the quantum channel with memory is indecomposable/forgetful, which roughly means that in the long term the behavior of the channel is independent of ρ^{S_0} (see [13], [14] for more details).

The changes that are necessary compared to Appendix D-A in order to estimate $I(X; Y)$, are shown in Eqs. (54)–(59) at the top of this page. The corresponding calculations are visualized in Figs. 16 and 18.

APPENDIX E SUPPLEMENTARY NOTES FOR SECTION IV

In this appendix we comment on Figs. 5–8. We start by commenting on the estimated information rate curves.

- Fig. 5: as is to be expected, the estimated information rate decreases for increasing p_b in the range $0 \leq p_b \leq 1/2$. This behavior continues for increasing p_b in the range

$1/2 \leq p_b \leq 1$. We conclude from this that the receiver has problems tracking the state for large p_b .

- Fig. 6: as is to be expected, the estimated information rate decreases for increasing p_b in the range $0 \leq p_b \leq 1/2$. This behavior continues only partly for increasing p_b in the range $1/2 \leq p_b \leq 1$. We conclude from this that when p_b approaches 1, the capabilities of the receiver to track the state improve again.
- Fig. 7: the larger α is in magnitude, the faster the channel state changes, thereby making it often more difficult for the receiver to track the state. (Note that the estimated information rate is not plotted for α of small magnitude because the channel is only slowly mixing for such α .)
- Fig. 8: similar comments apply here as for Fig. 7.

The estimated information rate lower bounds based on mismatched decoders nicely show the trade-off between computational complexity at the receiver side and achievable information rates. Interestingly, for some cases the (classical) 4-state-auxiliary-channel-based lower bound is rather close to the estimate information rate.

On the side, note that the estimation of the information rate lower bound based on a classical auxiliary channel with memory needs only typical input and output sequences \tilde{x}_1^n and \tilde{y}_1^n of the quantum channel with memory. The calculations are then done on an NFG representation of the classical auxiliary channel with memory (see [4], [9] for details). This is particularly interesting for scenarios where the simulation of the quantum channel with memory is too complicated on a classical computer, yet a physical realization of the quantum channel with memory is available.

Finally, let us point out that, from a practical point of view, we think that mismatched decoders based on classical auxiliary channels with memory will be even more important for quantum channels with memory than for classical channels with memory.

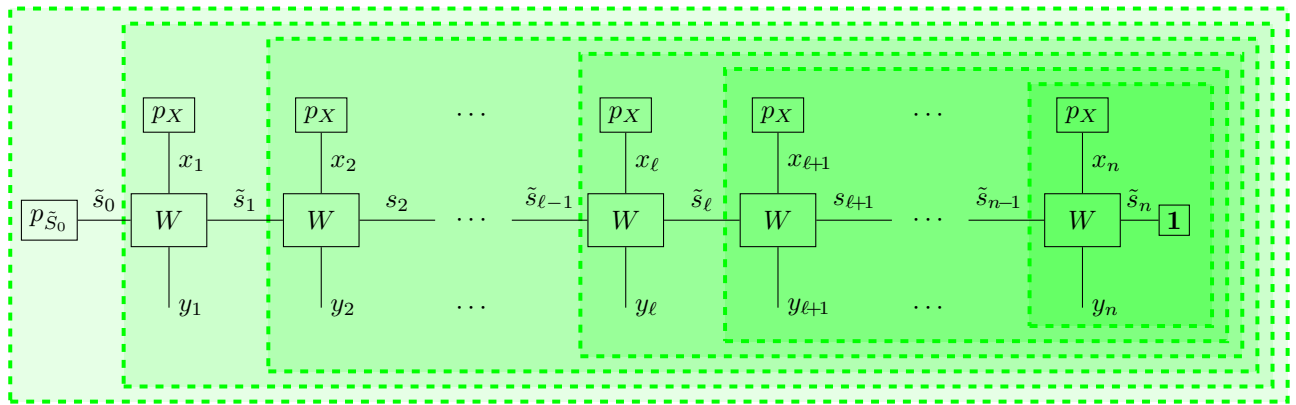


Fig. 11. Visualization of (16). Note that every closing-the-box operation yields a function node representing the constant function 1.

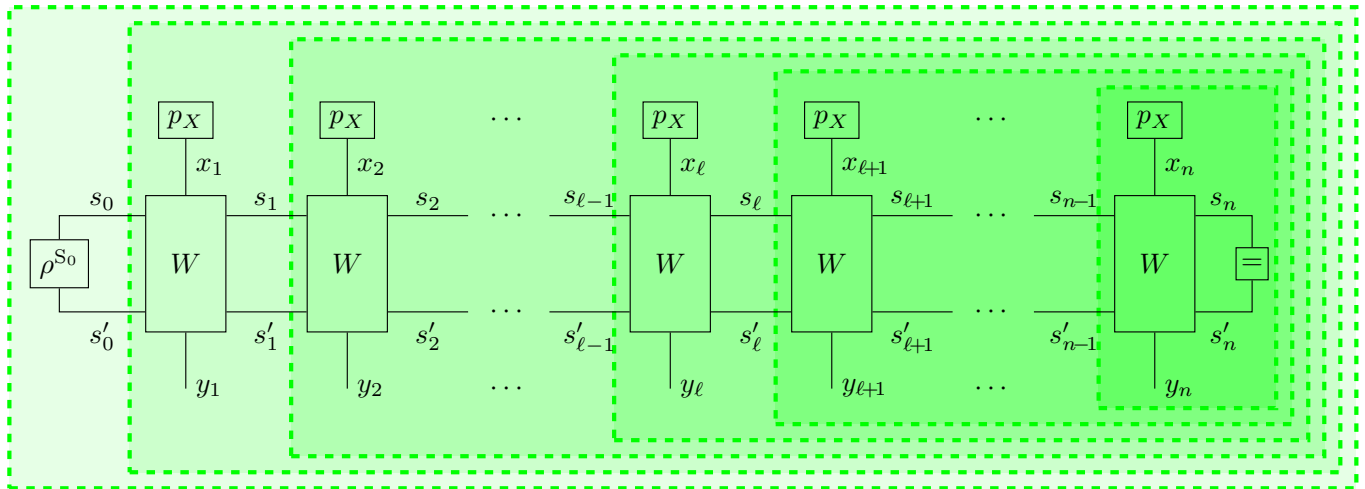


Fig. 12. Visualization of (22). Note that every closing-the-box operation yields a function node representing a Kronecker-delta function node, i.e., a degree-two equality function node.

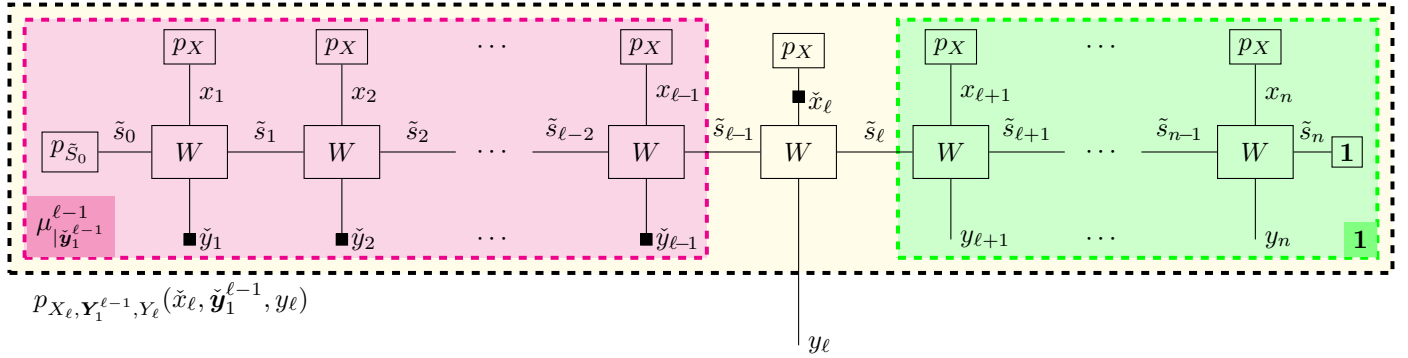


Fig. 13. Classical-channel-with-memory analog of the NFG in Fig. 14.

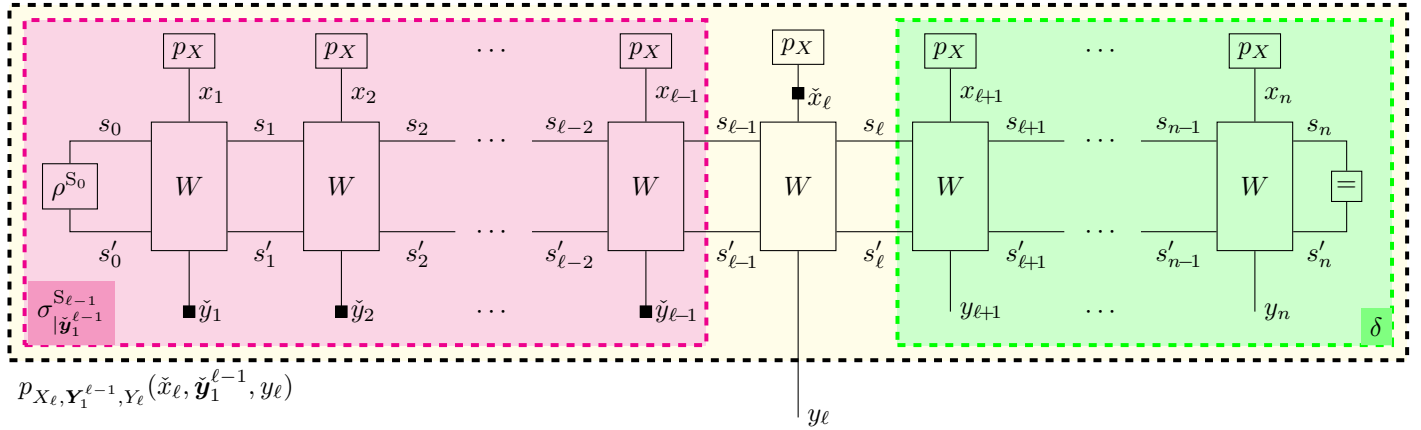


Fig. 14. Visualization of the computations in (37) via suitable closing-the-box operations. Note that applying the closing-the-box operation to the magenta box results in the function $\sigma_{\tilde{y}_1^{\ell-1}}^{s_{\ell-1}}(s_{\ell-1}, s'_{\ell-1})$, whereas applying the closing-the-box operation to the green box results in a Kronecker-delta function, *i.e.*, a degree-2 equality function node.

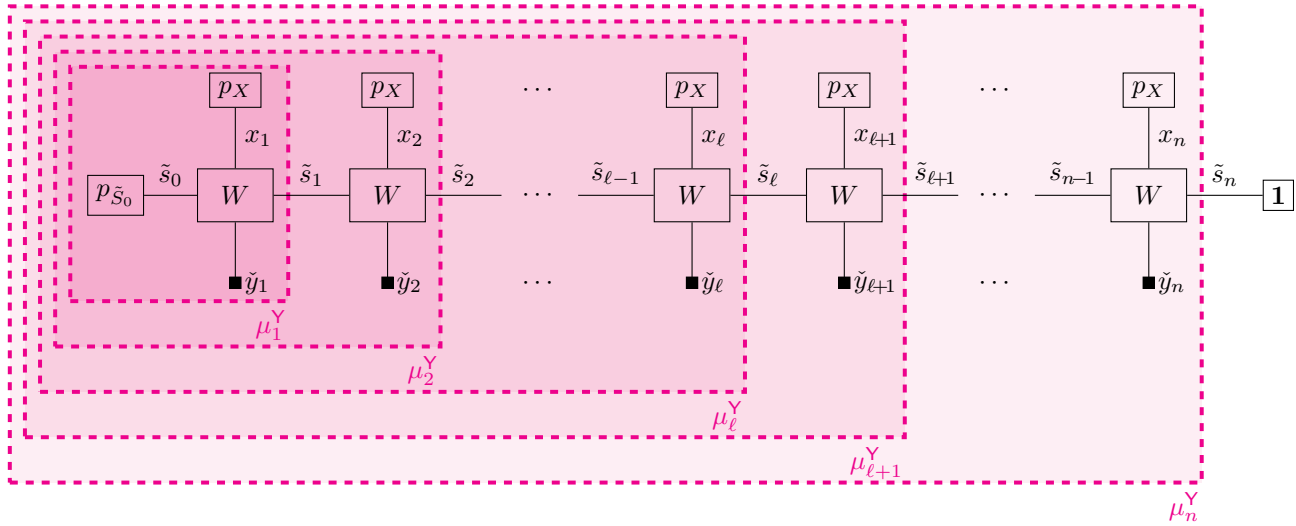


Fig. 15. The iterative computation of μ_ℓ^Y as described in (49) can be understood as a sequence of closing-the-box operations as shown above.

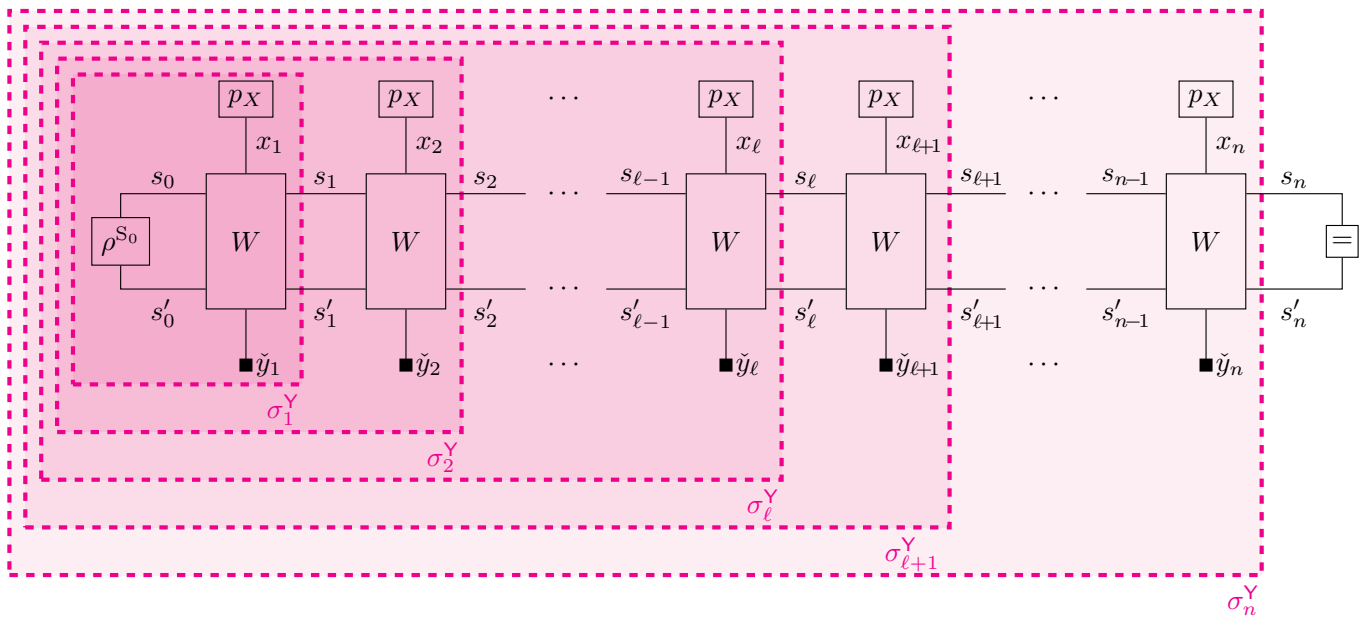


Fig. 16. The iterative computation of σ_ℓ^Y as described in (57) can be understood as a sequence of closing-the-box operations as shown above.

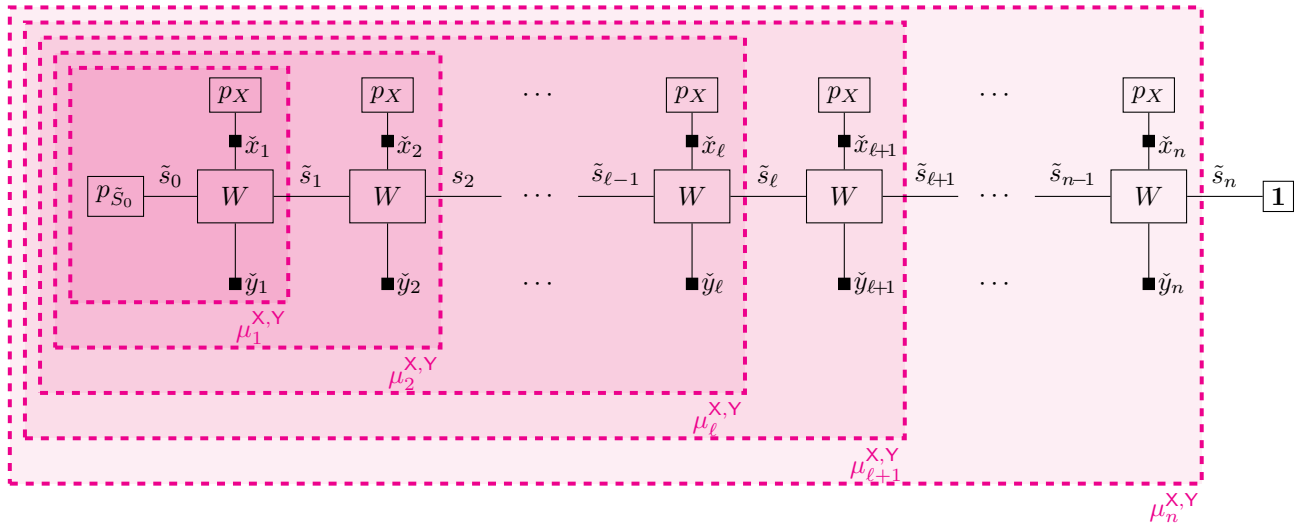


Fig. 17. The iterative computation of $\mu_{l+1}^{X,Y}$ can be understood as a sequence of closing-the-box operations as shown above.

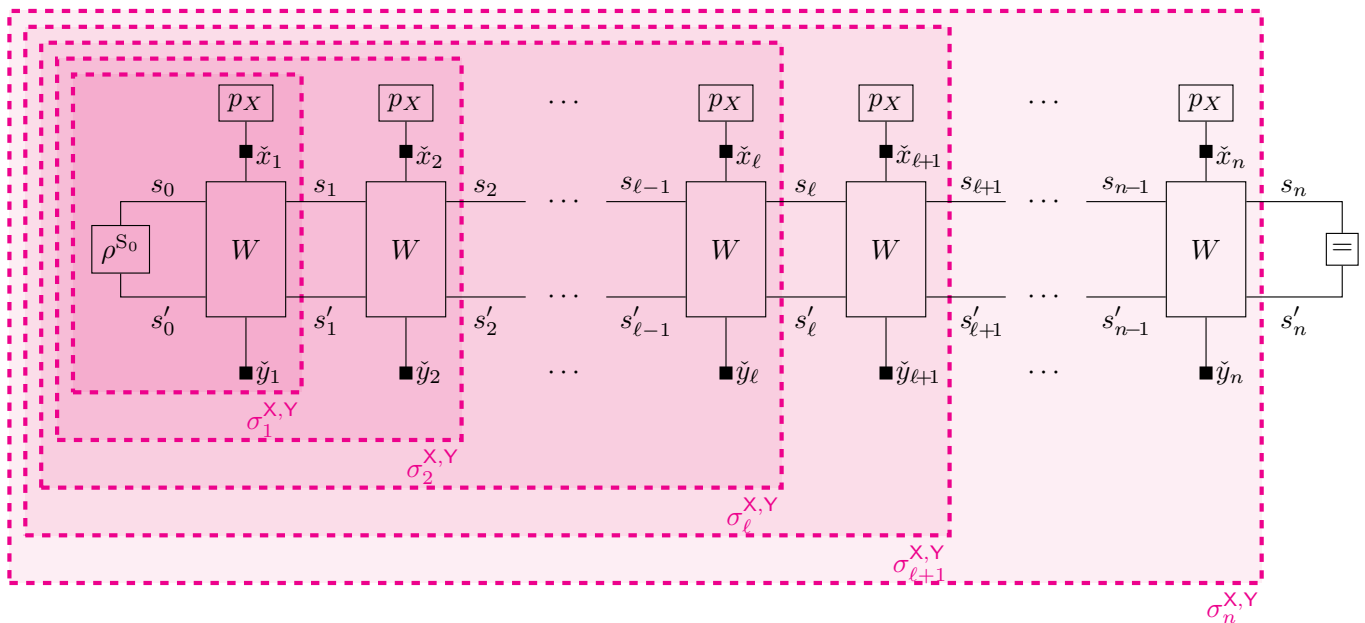


Fig. 18. The iterative computation of $\sigma_{l+1}^{X,Y}$ as described in (59) can be understood as a sequence of closing-the-box operations as shown above.